NISTIR 4726

Electronics and Electrical Engineering Laboratory

Technical Progress Bulletin

Covering Laboratory Programs,
July to September 1991,
with 1992 EEEL Events Calendar

U.S. DEPARTMENT OF COMMERCE
Technology Administration
National Institute of Standards and Technology
Electronics and Electrical Engineering Laboratory
Semiconductor Electronics Division
Gaithersburg, MD 20899

February 1992

91-3

U.S. DEPARTMENT OF COMMERCE
Robert A. Mosbacher, Secretary
NATIONAL INSTITUTE OF STANDARDS AND TECHNOLOGY
John W. Lyons, Director

NIST

NISTIR 4726

Electronics and Electrical Engineering Laboratory

Technical Progress Bulletin

Covering Laboratory Programs,
July to September 1991,
with 1992 EEEL Events Calendar

U.S. DEPARTMENT OF COMMERCE
Technology Administration
National Institute of Standards
and Technology
Electronics and Electrical
Engineering Laboratory
Semiconductor Electronics Division
Gaithersburg, MD 20899

February 1992

91-3

U.S. DEPARTMENT OF COMMERCE
Robert A. Mosbacher, Secretary
NATIONAL INSTITUTE OF STANDARDS
AND TECHNOLOGY
John W. Lyons, Director

INTRODUCTION TO FEBRUARY 1992 ISSUE OF THE EEEL TECHNICAL PROGRESS BULLETIN

This is the thirty-sixth issue of a quarterly publication providing information on the technical work of the National Institute of Standards and Technology Electronics and Electrical Engineering Laboratory (EEEL) (until February 1991, the Center for Electronics and Electrical Engineering). This issue of the EEEL Technical Progress Bulletin covers the third quarter of calendar year 1991.

Organization of Bulletin: This issue contains abstracts for all relevant papers released for publication by NIST in the quarter and citations and abstracts for such papers published in the quarter. Entries are arranged by technical topic as identified in the Table of Contents and alphabetically by first author under each subheading within each topic. Unpublished papers appear under the subheading "Released for Publication." Papers published in the quarter appear under the subheading "Recently Published." Following each abstract is the name and telephone number of the individual to contact for more information on the topic (usually the first author). This issue also includes a calendar of Laboratory conferences and workshops planned for calendar year 1992 and a list of sponsors of the work.

Electronics and Electrical Engineering Laboratory: EEEL programs provide national reference standards, measurement methods, supporting theory and data, and traceability to national standards. The metrological products of these programs aid economic growth by promoting equity and efficiency in the marketplace, by removing metrological barriers to improved productivity and innovation, by increasing U.S. competitiveness in international markets through facilitation of compliance with international agreements, and by providing technical bases for the development of voluntary standards for domestic and international trade. These metrological products also aid in the development of rational regulatory policy and promote efficient functioning of technical programs of the Government.

The work of the Laboratory is conducted by four technical research Divisions: the Semiconductor Electronics and the Electricity Divisions in Gaithersburg, Md., and the Electromagnetic Fields and Electromagnetic Technology Divisions in Boulder, Colo. In 1991, the Office of Law Enforcement Standards, formerly the Law Enforcement Standards Laboratory, was transferred to EEEL. This Office conducts research and provides technical services to the U.S. Department of Justice, State and local governments, and other agencies in support of law enforcement activities. In addition, the Office of Microelectronics Programs (OMP) was established in EEEL to coordinate the growing number of semiconductor-related research activities at NIST. Reports of work funded through the OMP are included under the heading "Semiconductor Microelectronics."

Key contacts in the Laboratory are given on the back cover; readers are encouraged to contact any of these individuals for further information. To request a subscription or for more information on the Bulletin, write to EEEL Technical Progress Bulletin, National Institute of Standards and Technology, Metrology Building, Room B-358, Gaithersburg, MD 20899 or call (301) 975-2220.

Laboratory Sponsors: The Laboratory Programs are sponsored by the National Institute of Standards and Technology and a number of other organizations, in both the Federal and private sectors; these are identified on page 33.

Note on Publication Lists: Publication lists covering the work of each division are guides to earlier as well as recent work. These lists are revised and reissued on an approximately annual basis and are available from the originating division. The current set is identified in the Additional Information section, page 30.

TABLE OF CONTENTS

FUNDAMENTAL ELECTRICAL MEASUREMENTS

Released for Publication

Pieper, J., Price, J., and Martinis, J.M., **Frequency Dependence of Weak Localization in Disordered Ag Wires.**

We have measured the complex magnetoconductance of disordered Ag wires at 1 GHz and 1.6 K. The wires are in the quasi-one-dimensional limit for weak localization. Magnetoconductance measurements at dc were also made to characterize the samples. A frequency dependence of the weak localization conductance is visible at 1 GHz because this frequency is of the same order as the dominant dephasing rate in the sample. A new imaginary part to the magnetoconductance is seen which is in very good agreement with theory. The measurements provide an accurate value for the electron diffusion constant, which cannot be obtained from dc weak localization experiments. These data provide a first test of the theory of weak localization at finite frequency, due originally to Gor'kov, Larkin, and Khmel'nitskii.
[Contact: John M. Martinis, (303) 497-3597]

Van Degrift, C.T., Yoshihiro, K., Cage, M.E., Yu, D., Segawa, K., Kinoshita, J., and Endo, T., **Anomalously Offset Quantized Hall Plateaus in High Mobility Si-MOSFETs,** to be published in the Proceedings of the Electronic Properties of Two-Dimensional Electron Systems Conference, Nara, Japan, July 8-12, 1991. (Conference Proceedings to be published in Surface Science 1992.)

Measurements made using two independent, high-precision systems on different samples of high-mobility silicon-MOSFETs have revealed unexpected irregularities in their i=4 quantized Hall plateaus in spite of exceedingly low diagonal resistivities, 0.002 parts per million of the plateau value. Relatively flat, metastable plateaus were observed which were offset by up to 0.4 parts per million above the corresponding GaAs/AlGaAs value under the measurements at 14 to 14.5 T, 0.34 to 0.5 K, with about 10-μA sample current. Possible connection of these phenomena with the offset plateaus observed by Kawaji et al. is discussed. At present, no satisfactory explanation has been provided for these phenomena.
[Contact: Craig T. Van Degrift, (301) 975-4248]

Recently Published

Olsen, P.T., Tew, W.L., Williams, E.R., Elmquist, R.E., and Sasaki, H., **Monitoring the Mass Standard via the Comparison of Mechanical to Electrical Power,** IEEE Transactions on Instrumentation and Measurement (Special Issue of selected papers, CPEM '90), Vol. 40, No. 2, pp. 115-120 (April 1991). [Also published in the Digest of the 1990 Conference on Precision Electromagnetic Measurements, Ottawa, Canada, June 11-14, 1990, pp. 180-181 (1990).]

This paper presents the current status of the NIST SI watt experiment. Included are goals for the near future as well as projections regarding the viability of monitoring and/or replacing the kilogram mass standard. Although several significant systematic errors have yet to be evaluated, the standard deviation of the mean of our present measurement distributions is 0.05 parts per million.
[Contact: P. Thomas Olsen, (301) 975-6553]

Tew, W.L., Olsen, P.T., and Williams, E.R., **The Use of Magnetic Forces in the Alignment of a Radial Field Superconducting Magnet,** Abstract, Proceedings of the 5th Joint Magnetism and Magnetic Materials - Intermag Conference, Pittsburgh, Pennsylvania, June 18-21, 1991, pp. 93-94 (June 1991).

A detailed description of the forces between a special radial field superconducting magnet and a suspended current-carrying coil is given. A primary vertical force is used directly in the determination of the SI watt. In addition, small nonvertical forces and torques are monitored to determine the magnetic alignment stability. Results are compared with calculations.
[Contact: Weston L. Tew, (301) 975-6552]

SEMICONDUCTOR MICROELECTRONICS

Compound Materials

Released for Publication

Bennett, H.S., and Lowney, J.R., **Experimentally Verified Majority and Minority Mobilities in Heavily Doped GaAs for Device Simulations.**

Low-field mobilities and velocity-versus-electric-field

relations are among the key input parameters for drift-diffusion simulations of field-effect and bipolar transistors. For example, most device simulations that treat scattering from ionized impurities contain mobilities or velocity-versus-field relations based on the Born approximation (BA). The BA is insensitive to the sign of the charged impurity and is especially poor for ionized impurity scattering because of the relatively strong scattering of long-wavelength carriers, which have low energies, and therefore violate the validity condition for the BA. Such carriers occur at high symmetry points in the Brillouin zone and are critical for device behavior.

There has been a tendency in the past to assume that majority and minority mobilities are equal. This assumption can lead to incorrect interpretations of device data, thereby misleading design strategies based on such simulations. We have calculated the majority electron and minority hole mobilities in GaAs at 300 K for donor densities between 5×10^{16} and 1×10^{19} cm^{-3} and the majority hole and minority electron mobilities for acceptor densities between 5×10^{16} and 1×10^{20} cm^{-3}. We have included all the important scattering mechanisms for GaAs: acoustic phonon, polar optic phonon, nonpolar optic phonon (holes only), piezoelectric, ionized impurity, carrier-carrier, and plasmon scattering.

The ionized impurity and carrier-carrier scattering processes have been calculated with a quantum mechanical phase-shift analysis to obtain more accurate matrix elements for these two scattering mechanism. We compare the total scattering rate for majority electrons due to ionized impurities based on exact phase shifts and on the BA of Brooks-Herring. We also present additional data that show the differences between the exact phase-shift analyses and the BA for majority electron scattering rates as functions of carrier energy and scattering angle. These results show that the calculated low-field mobilities are in good agreement with experiment, but they predict that at high dopant densities, minority mobilities should increase with increasing dopant density for a short range of densities. This effect occurs because of the reduction of plasmon scattering and the removal of carriers from carrier-carrier scattering because of the Pauli exclusion principle. Some recent experiments support this finding. These results are important for device modeling because of the need to have reliable values for the minority mobilities and velocity-field relations.

[Contact: Herbert S. Bennett, (301) 975-2047]

DeSalvo, G.C., Tseng, W.F., and Comas, J., **Etch Rates and Selectivities of Citric Acid/Hydrogen Peroxide on GaAs, $Al_{.3}Ga_{.7}As$, $In_{.2}Ga_{.8}As$, $In_{.53}Ga_{.47}As$, $In_{.52}Al_{.48}As$, and InP.**

Investigation of citric acid/hydrogen peroxide ($C_6H_8O_7/H_2O_2$) at volume ratios from 0.5 to 50 were found to provide good selective etching of various III-V semiconductor materials grown on GaAs and InP substrates. Choosing different volume ratios of citric acid/hydrogen peroxide provides both selective and uniform (nonselective) etching regions. Etchant selectivities of the GaAs-based materials were measured to be as high as 110 for $GaAs/Al_{.3}Ga_{.7}As$ and 120 for $In_{.2}Ga_{.8}As/Al_{.3}Ga_{.7}As$. In addition, the InP system had selectivities of approximately 60 and 80 for $In_{.53}Ga_{.47}As/In_{.52}Al_{.48}As$ and $In_{.52}Al_{.48}As/InP$, with the highest selectivity of 473 found for $In_{.53}Ga_{.47}As/InP$. The $C_6H_8O_7/H_2O_2$ system can be used as a stop etch for InP-based devices, as InP is virtually unaffected by this etchant. Finally, citric acid/hydrogen peroxide can be used to preferentially etch these materials through a photoresist mask, since it does not erode photoresist at any volume ratio.

[Contact: Gregory C. DeSalvo, (301) 975-2135]

Hadjipanteli, S., Iliadis, A.A., Comas, J., and Pellegrino, J.G., **The Effects of Indium Doping on the M and EL Centers in GaAs Grown by MBE.**

A series of GaAs layers grown by molecular-beam epitaxy at relatively low growth temperatures (530 °C) and doped with In at levels between 0% and 6.6% were studied by deep-level transient spectroscopy, Hall effect measurement, X-ray analysis, and I-V and C-V measurements. It is demonstrated that for the conditions of our growth, an optimum level of In at 0.1% reduced the density of the well-known M centers below $10^{11}cm^{-3}$ but left unaffected an EL center. The EL center, observed for the first time in In-doped GaAs, is speculated to be related to the EL2 center. It was concluded that high-quality GaAs can be obtained at relatively low temperatures by incorporating the appropriate amounts in In.

[Contact: James Comas, (301) 975-2061]

Recently Published

Seiler, D.G., Lowney, J.R., Littler, C.L., Yoon, I.T., and Loloee, M.R., **Photoexcited Hot Electron Relaxation Processes in n-HgCdTe Through Impact Ionization Into Traps**, Journal of Vacuum Science Technology B, Vol. 9, No. 3, pp. 1847-1851 (May/Jun 1991). [Also published in American Vacuum Society Series 11, Physics and Chemistry of Mercury Cadmium Telluride and Novel IR Detector Materials, pp. 1847-1851 (American Institute of Physics, New York, 1991, D.G. Seiler, Ed.) (Proceedings of the 1990 U.S. Workshop on the Physics and Chemistry of Mercury Cadmium Telluride and Novel Infrared Detector Materials, San Francisco, California, October 2-4, 1990).]

In this paper we report on a new type of spectroscopy for impurity and/or defect levels in the energy gap of narrow-gap semiconductors using the near-band-gap photon energies from a laser. This spectroscopy is done under the conditions of intense laser photoexcitation and is associated with the Auger relaxation processes of hot electrons involving impact ionization of valence electrons into impurity or defect levels. Wavelength-independent structure in the photoconductive response versus magnetic field is observed at high intensities in samples of $Hg_{1-x}Cd_xTe$ with $x \approx 0.22$ and 0.24. This structure arises from hot electrons photoexcited high into the conduction band by sequential absorption of CO_2 laser radiation. The hot electrons lose their energy by impact-ionizing valence electrons into impurity/defect levels in the gap. For the sample with $x \approx 0.22$ and an energy gap of 95 meV, three levels are found at 15, 45, and 59 meV above the valence band. A level at 61 meV is found for the sample with $x \approx 0.24$ and a gap of 122 meV. [Contact: David G. Seiler, (301) 975-2081]

Zawadzki, W., Song, X.N., Littler, C.L., and Seller, D.G, **High Excited States of Magnetodonors in InSb: An Experimental and Theoretical Study** [original title: High Excited States of Magneto-Donors in InSb: Experimental and Theoretical Study], Physical Review B, Vol. 42, No. 8, pp. 5260-5269 (15 September 1990).

New optical transitions between magnetodonor states in InSb assisted by optic-phonon emission have been observed and described theoretically. Photoconductive detection and magnetic-field modulation were used to obtain well-resolved magneto-optical data. Phonon-assisted excitations provide a unique opportunity to investigate high excited states of the magnetodonor system (up to principal quantum number n = 13), which simulates the hydrogen atom in gigantic magnetic fields. The magnetodonor states have been described variationally, taking into account the narrow energy gap and the spin-orbit interaction of the band structure of InSb. It has been shown how the phonon emission breaks the selection rules for the magneto-optical excitations, allowing for transitions with large Δn. Good agreement between theory and experiment has been obtained. The results should also be of importance to atomic physics and astrophysics. [Contact: David G. Seller, (301) 975-2081]

Analysis Techniques

Released for Publication

Kopanski, J.J., Carver, G.P., Lowney, J.R., Miles, D.S., and Novotny, D.B., **High Spatial Resolution Mapping of Resistivity Variations in Semiconductors.**

A new approach to the mapping of resistivity variations in semiconductors uses probe sites provided by an array of lithographically defined contacts with a density of 60,000 sites per cm^2. One- or two-probe spreading resistance or four-point-probe resistance measurements can be made. Solutions of the Laplace equation and measurements on silicon that had been ion-implanted to form abrupt boundaries in resistivity are used to show that the spatial resolution of the technique is determined primarily by the spacing of the measurement sites, not by the spreading of the current from the contacts. The technique has been implemented with a resolution of lateral variations in resistivity of 45 μm in width and ±5% in magnitude from the background resistivity. As an example application, a study of the resistivity variations of a silicon boule with pronounced growth striations is presented.
[Contact: Joseph J. Kopanski, (301) 975-2059]

Device Physics and Modeling

Released for Publication

Bennett, H.S., and Lowney, J.R., **Experimentally Verified Majority and Minority Mobilities in Heavily**

Doped GaAs for Device Simulations.

Low-field mobilities and velocity-versus-electric-field relations are among the key input parameters for drift-diffusion simulations of field-effect and bipolar transistors. For example, most device simulations that treat scattering from ionized impurities contain mobilities or velocity-versus-field relations based on the Born approximation (BA). The BA is insensitive to the sign of the charged impurity and is especially poor for ionized impurity scattering because of the relatively strong scattering of long-wavelength carriers, which have low energies, and therefore violate the validity condition for the BA. Such carriers occur at high symmetry points in the Brillouin zone and are critical for device behavior.

There has been a tendency in the past to assume that majority and minority mobilities are equal. This assumption can lead to incorrect interpretations of device data, thereby misleading design strategies based on such simulations. We have calculated the majority electron and minority hole mobilities in GaAs at 300 K for donor densities between 5×10^{16} and 1×10^{19} cm^{-3} and the majority hole and minority electron mobilities for acceptor densities between 5×10^{16} and 1×10^{20} cm^{-3}. We have included all the important scattering mechanisms for GaAs: acoustic phonon, polar optic phonon, nonpolar optic phonon (holes only), piezoelectric, ionized impurity, carrier-carrier, and plasmon scattering.

The ionized impurity and carrier-carrier scattering processes have been calculated with a quantum mechanical phase-shift analysis to obtain more accurate matrix elements for these two scattering mechanism. We compare the total scattering rate for majority electrons due to ionized impurities based on exact phase shifts and on the BA of Brooks-Herring. We also present additional data that show the differences between the exact phase-shift analyses and the BA for majority electron scattering rates as functions of carrier energy and scattering angle. These results show that the calculated low-field mobilities are in good agreement with experiment, but they predict that at high dopant densities, minority mobilities should increase with increasing dopant density for a short range of densities. This effect occurs because of the reduction of plasmon scattering and the removal of carriers from carrier-carrier scattering because of the Pauli exclusion principle. Some recent experiments support this finding. These results are important for device modeling because of the need to have reliable values for the minority mobilities and velocity-field relations.

[Contact: Herbert S. Bennett, (301) 975-2047]

Bennett, H.S., and Lowney, J.R., **Physics for Device Simulations and Its Verification by Measurements,** to be published in the Proceedings of the Summer Program on Semiconductors of the Institute for Mathematics and Its Applications, Minneapolis, Minnesota, July 22-August 2, 1991.

The motivations for using computers to simulate the electrical characteristics of transistors are discussed. Our work and that of others in the area of device physics and modeling are described. We compare conventional device physics with an alternative approach to device physics that is more directly traceable to quantum-mechanical concepts. We then apply this new approach to quasi-neutral regions, space-charge regions, and regions with high levels of carrier injection. Examples of applying quantum-mechanically-based device physics to energy band diagrams for bipolar transistors are given. The limits for using theoretical results from uniform media in numerical simulations of devices with large concentration gradients are discussed. Calculations of the effective intrinsic carrier concentrations for gallium arsenide and silicon are also given along with published data. In addition, calculations of the mobilities for GaAs that are based in part on quantum-mechanical phase shifts are compared with published data. We then conclude with a discussion of the requirements for verifying and calibrating device simulators for the submicrometer domain.

[Contact: Herbert S. Bennett, (301) 975-2053]

Lowney, J.R., and Mayo, S., **Analysis of Persistent Photoconductivity Due to Potential Barriers,** to be published in the Proceedings of the 3rd Workshop on Radiation-Induced and/or Process-Related Electrically Active Defects in Semiconductor-Insulator Systems, Research Triangle Park, North Carolina, September 10-13, 1991.

Persistent photoconductivity has been seen in thin silicon resistors fabricated with SIMOX material at temperatures between 60 and 220 K. This effect has

been attributed to the depletion of carriers near the interface between the top silicon layer and the buried oxide, which is due to the large number of surface traps at this interface. The depletion of carriers is accompanied by a built-in field on the order of 10,000 V/cm, which causes a potential barrier that is about a quarter of the energy gap of silicon. The theory of the recombination kinetics of majority carriers with minority carriers trapped at the interface on the other side of a potential barrier is studied. Both the possibilities of tunneling and thermal activation have been considered. The results show that thermal activation dominates at the temperatures of the NIST measurements in SIMOX material, while at lower temperatures tunneling would dominate.
[Contact: Jeremiah R. Lowney, (301) 975-2048]

Recently Published

Geist, J., Lowney, J.R., James, C.R., and Robinson, A.M., **Testing the Accuracy of Calculated Equilibrium Carrier Concentrations in the Presence of Surface Fields** (original title: Accuracy of Numerical Techniques in Calculating Equilibrium Carrier Concentrations in the Presence of Surface Fields], Journal of Applied Physics, Vol. 70, No. 1, pp. 236-242 (1 July 1991).

Simple analytic expressions for the one-dimensional, majority-carrier concentration in a uniformly doped, semi-infinite semiconductor with a charge-accumulated front surface are derived. These expressions are based on the assumption that the effective intrinsic carrier concentration depends only upon the concentration of the majority dopant. Within the framework of this assumption, the expressions derived here are rigorously accurate for intrinsic material, and are accurate to well within 100 parts per million for doping concentrations about 10^{12} cm^{-3}. The results of calculations of the majority-carrier concentration carried out using these expressions and using a widely available one-dimensional semiconductor device modeling program are compared to illustrate how these expressions are used for testing the accuracy of iterative solutions of the drift-diffusion equations in the presence of surface fields.
[Contact: Jon Geist, (301) 975-2066]

Hefner, A.R., Jr., and Diebolt, D.M., **An Experimentally Verified IGBT Model Implemented in the Saber Circuit Simulator**, PESC '91 Record, 22nd Annual IEEE Power Electronics Specialist Conference, Cambridge, Massachusetts, June 24-27, 1991, pp. 10-19 (1991).

A physics-based Insulated Gate Bipolar Transistor (IGBT) model is implemented into the general purpose circuit simulator Saber. The IGBT model includes all of the physical effects that have been shown to be important for describing IGBTs, and the model is valid for general external circuit conditions. The Saber IGBT model is evaluated for the range of static and dynamic conditions in which the device is intended to be operated, and the simulations compare well with experimental results for all of the conditions studied.
[Contact: Allen R. Hefner, Jr., (301) 975-2071]

Insulators and Interfaces

Released for Publication

Witczak, S.C., Suehle, J.S., Gaitan, M., and Yang, C.H., **An Experimental Comparison of Measurement Techniques to Extract Si-SiO_2 Interface Trap Density.**

For the first time, five methods of measuring Si-SiO_2 interface trap densities were compared on three otherwise identical MOSFETs which were radiation-stressed so as to induce different levels of interface trap densities. The results show that when sources of error and limitations are taken into account, these methods capable of estimating interface trap densities are in good quantitative agreement. Furthermore, the change in measured interface trap densities with radiation is independent of the method used. A comprehensive review of the methods is presented.
[Contact: John S. Suehle, (301) 975-2243]

Recently Published

Krause, S.J., Visitserngtrakul, S., Cordts, B.F., and Roitman, P., **Microstructural Evolution of Oxides During Processing of Oxygen Implanted SOI Material**, Extended Abstract, Proceedings of the 1990 IEEE SOS/SOI Technology Conference, Key West, Florida, October 2-4, 1990, pp. 47-48 (1990).

Silicon-on-insulator (SOI) material fabricated by oxygen implantation (SIMOX) is being used for radiation-hard, higher speed, and higher temperature

integrated circuits. The microstructural evolution of oxides during implantation, thermal ramping, and annealing plays a crucial role in development of the structure of the top Si layer and of the buried oxide layer. To control the microstructure of the oxides and silicon, it is necessary to understand the effect of processing conditions on the mechanisms of oxide formation and evolution. These processing conditions include: implantation temperature, energy, and dose; thermal ramping rate; and annealing time, temperature, and atmosphere. Numerous questions still remain on the effects of processing conditions and include: formation and growth of the buried oxide; formation and evolution of oxygen bubbles in the top silicon layer; and precipitate evolution and elimination during ramping and annealing. The goal of this paper is to summarize recent work on the effects of processing conditions on oxide evolution and to present new results on effects of implantation conditions on buried oxide formation, effects of ramping conditions on oxygen bubble evolution and defect formation, and effects of annealing conditions on the structure of the buried oxide and its interfaces.
[Contact: Peter Roitman, (301) 975-2077]

Roitman, P., Simons, D.S., Visitserngtrakul, S., Jung, C.O., and Krause, S.J., **Effect of Annealing Ambient on the Precipitation Processes in Oxygen-Implanted Silicon-on-Insulator Material**, Extended Abstract, Proceedings of the XIIth International Congress for Electron Microscopy, Seattle, Washington, August 12-17, 1990, Vol. 4, L.D. Peachey and D.B. Williams, Eds., pp. 644-645 (1990).

In the last decade, oxygen-implanted silicon-on-insulator material (SIMOX: separation by IMplantation of OXygen) has been extensively studied, due to its potential advantages of increased speed and radiation hardness in integrated circuits. SIMOX material requires two processing steps: first, implantation of a high dose of oxygen to form a buried oxide layer below a thin, top silicon layer, and second, a high-temperature anneal in an inert gas atmosphere to remove implantation damage and oxide precipitates. Most earlier studies investigated the effect of annealing temperature and time, but did not consider the effect of gas ambient. The effect of nitrogen and argon on the oxide-precipitate formation in bulk silicon has been established. Raider et al. found that in annealing of bulk silicon, nitrogen can diffuse to an oxide-silicon interface and chemically react with silicon. The nitrogen-containing layer acts as a barrier to further oxidation. Consequently, nitrogen influences the growth kinetics of the thermal oxide, while annealing in an argon ambient does not. This should apply to SIMOX as well. We have, therefore, investigated the effect of nitrogen and argon ambient on the oxide-precipitate removal during annealing of SIMOX material.
[Contact: Peter Roitman, (301) 975-2077]

Dimensional Metrology

Recently Published

Mattis, R.L, **The NIST Linewidth Measurement Program**, SRC Newsletter, Vol. 9, No. 9, pp. 4-5 (September 1991).

The NIST linewidth measurement program has produced several photomask linewidth standards. While continuing development of these standards, the Precision Engineering Division is working on optical overlay measurement, optical modeling, and length standards to be used with scanning electron microscopes.
[Contact: Richard L. Mattis, (301) 975-2235]

Integrated-Circuit Test Structures

Released for Publication

Allen, R.A., and Cresswell, M.W., **Elimination of Effects Due to Patterning Imperfections in Electrical Test Structures for Submicrometer Feature Metrology.**

This paper describes the elimination of a substrate-dependent systematic error that was experienced in prior work: on measuring the separation of parallel features with total errors less than 10 nm with an electrical test structure. The test structure was an enhancement of a sliding-wire voltage-dividing potentiometer which scaled the overall test structure geometry to obtain greater sensitivity. It also incorporated features to eliminate adverse effects of voltage tap- and bridge-linewidth scaling. The measurement algorithm that was developed provided the relative separations of sets of features to the 10 nm-level. However, absolute measurements were offset by a

quantity characteristic of the substrate from which they were extracted. The evidence suggested that these systematic errors were not caused by the primary pattern generation tool. Through observations, measurements, and simulations, this paper attributes the substrate-characteristic systematic error to an orientation dependence of the quality of the replication of certain features of the test structure. An alternative design and measurement algorithm is shown to be able to greatly reduce the errors.
[Contact: Richard A. Allen, (301) 975-5026]

Marshall, J.C., and Mattis, R.L., **Evaluating a Chip, Wafer, or Lot Using SUXES, SPICE, and STAT2**, to be published as NIST Special Publication 400-90.

To facilitate integrated circuit evaluation for a chip, wafer, or lot, the computer procedure KEYS was written. KEYS links SUXES, SPICE, and STAT2. Given data points for individual devices, SUXES obtains the model parameters for SPICE. SPICE predicts the behavior of an individual device or an entire circuit. After analyzing each test chip on a wafer, STAT2 determines the correlation coefficients and generates wafer maps of selected parameters. These wafer maps are valuable to the designer, modeler, and process engineer.

The entire package accomplishes the following: (1) standardizes the technique of running SUXES and SPICE; (2) simulates and plots the characteristic curves; (3) simulates and plots the results of an optional dynamic circuit (for example, a ring oscillator); (4) does steps (2) and (3) for every test chip on each wafer; (5) summarizes the results from each chip, each wafer, and the lot; (6) rank-orders the parameters for each wafer according to their correlation coefficients with respect to chosen parameters; and (7) generates wafer maps of several quantities. A CMOS 19-stage ring oscillator is used to illustrate the capabilities of KEYS.
[Contact: Janet C. Marshall, (301) 975-2049]

Schuster, C.E., Linholm, L.W., and Gillespie, J.K., **High Density Test Structures for Assessing MIMIC Performance**, to be published in the 1991 Digest of Papers, Proceedings of the 1991 Government Applications Conference (GOMAC), Orlando, Florida, November 5-7, 1991.

This paper discusses the unique, high-density implementation of microelectronic test structures used to diagnose and predict MIMIC performance under MIMIC Phase 1, Task 4.E. It also presents assessments and recommendations, based on Task 4.E data, to improve and extend current parametric test structure methods for use in future efforts to correlate and monitor MIMIC material, process, and device characteristics.
[Contact: Constance E. Schuster, (301) 975-2241]

Recently Published

Suehle, J.S., and Galloway, K.F., **The Effects of Localized Hot-Carrier-Induced Charge in VLSI Switching Circuits**, Microelectronics Journal, Vol. 21, No. 3, pp. 5-14, (1990). [Also to be published in the Proceedings of the 17th Yugoslav Conference on Microelectronics.]

This paper presents data collected from CMOS test circuits designed to characterize hot-carrier effects in digital switching circuits. Test circuits were configured as CMOS inverters, transmission gates, and NMOS transmission gates. The MOSFETs within the circuits could be probed so that the degradation of their dc characteristics could be directly measured These circuits were hot-carrier-stressed under pulsed switching conditions similar to their operation in VLSI circuits. The results indicate that device degradation is strongly dependent on the circuit configuration and switching conditions. Transmission gate circuits exhibit a more severe degradation in switching characteristics than inverter circuits due to the localization of the hot-carrier-induced charge. The localized nature of hot-carrier-induced charge must be considered at the circuit simulation level to accurately assess the effect on circuit performance.
[Contact: John S. Suehle, (301) 975-2247]

Plasma Processing

Released for Publication

Olthoff, J.K., Roberts, J.R., Van Brunt, R.J., Whetstone, J.R., Sobolewski, H.A., and Djurovic, S., **Mass Spectrometric and Optical Emission Diagnostics for rf Plasma Reactors**, to be published in the Proceedings of SPIE (The International Society for Optical Engineering, P.O. Box 10, Bellingham, Washington 98227-0010), Technical Symposium on

Microelectronic Processing Integration '91, San Jose, California, September 9-13, 1991.

Mass spectrometric and optical emission studies have been performed on argon discharges in a parallel-plate rf reactor. Ion energy distributions exhibit structure for ions produced in the sheath region, while ions produced in the bulk plasma exhibit narrow energy distribution indicative of the sheath potential. The addition of small amounts of O_2 to an argon discharge significantly alters the observed ion energy distributions. Optical emission studies indicate increasing spatial nonuniformity in the plasma at higher pressures. Time-resolved optical emission studies indicate a varying relationship between the applied rf voltage and the time-varying optical emission with changing pressure and position between the electrodes.
[Contact: James K. Olthoff, (301) 975-2431]

Recently Published

Olthoff, J.K., Van Brunt, R.J., Wan, H.X., and Moore, J.H., **Electron Attachment to SF_6 and SO_2**, Program of the Joint Symposium on Electron and Ion Swarms and Low Energy Electron Scattering, Queensland, Australia, July 18-20, 1991, pp. 25-27 (1991).

SF_6 is a favorable gas for use in the plasma etching of microelectronic devices. However, SF_6 plasmas are complex because of the large number of secondary products that are formed by reactions with oxygen and trace amounts of water. Under some etching conditions, the mole fraction of stable decomposition products in an SF_6/O_2 plasma can exceed 20% of the neutral species. A full understanding of the physical processes occurring in SF_6 discharges requires a detailed knowledge of the interaction of low-energy electrons with SF_6 and its electrical discharge by-products. We have measured absolute cross sections for electron scattering and for negative ion formation through electron attachment to SF_6 and to several by-products (SO_2, SOF_2, SO_2F_2, SOF_4, and SF_4) produced by electrical discharges in SF_6. Due to space limitations, only the results for SF_6 and SO_2 are presented in this abstract. Preliminary results of these measurements were presented previously and are now superseded by the cross sections presented here.
[Contact: James K. Olthoff, (301) 975 2431]

Radovanov, S.B., Olthoff, J.K., and Van Brunt, R.J., **Off-Axis Measurements of Ion Kinetic Energies in RF Plasmas**, Proceedings of the XX International Conference on Phenomena in Ionized Gases, Barga, Italy, July 8-12, 1991, pp. 835-836 (Instituto di Fisica Atomica, Pisa, Italy, 1991).

Ion kinetic energy distributions are presented for argon plasmas in the GEC radiofrequency reference cell (developed by the Gaseous Electronics Conference - GEC) and are compared with other previous measurements.
[Contact: James K. Olthoff, (301) 975-2431]

Power Devices

Released for Publication

Blackburn, D.L., **Failure Mechanisms and Nondestructive Testing of Power Bipolar and MOS-Gated Transistors**, to be published in the Proceedings of the Symposium on Materials and Devices for Power Electronics, Florence, Italy, September 2-6, 1991.

Failure mechanisms and nondestructive testing of power bipolar and MOS-gated devices are discussed. Bipolar transistor failures are initiated at relatively low temperatures, and these devices can be tested nondestructively. Modern MOS-gated device failure is initiated at temperatures far in excess of those normally considered safe and cannot be tested nondestructively today. The key to nondestructive testing is the ability to sense the onset of failure and to then remove all power from the transistor before the device temperature rises high enough to cause damage.
[Contact: David L. Blackburn, (301) 975-2068]

Photodetectors

Recently Published

Geist, J., Chandler-Horowitz D., Robinson, A.M., and James, C.R., **Numerical Modeling of Silicon Photodiodes for High-Accuracy Applications. Part I: Simulation Programs**, Journal of Research of the National Institute of Standards and Technology, Vol. 96, No. 4, pp. 463-469 (July-August 1991).

The suitability of the semiconductor-device modeling

program PC-1D for high-accuracy simulation of silicon photodiodes is discussed. A set of user interface programs optimized to support high-accuracy batch-mode operation of PC-1D for modeling the internal quantum efficiency of photodiodes is also described. The optimization includes correction for the dark current under reverse and forward bias conditions before calculating the quantum efficiency, and easy access to the highest numerical accuracy available from PC-1D, neither of which are conveniently available with PC-1D's standard user interface.
[Contact: Jon Geist, (301) 975-2066]

Geist, J., Kohler, R., Goebel, R., Robinson, A.M., and James, C.R., **Numerical Modeling of Silicon Photodiodes for High-Accuracy Applications. Part II: Interpreting Oxide-Bias Experiments,** Journal of Research of the National Institute of Standards and Technology, Vol. 96, No. 4, pp. 471-479 (July-August 1991).

The semiconductor device modeling program PC-1D and the programs that support its use in high-accuracy modeling of photodiodes, all of which were described in Part I of this paper, are used to simulate oxide-bias self-calibration experiments on three different types of silicon photodiodes. It is shown that these simulations can be used to determine photodiode characteristics, including the internal quantum efficiency for the different types of photodiodes. In the latter case, the simulations provide more accurate values than can be determined by using the conventional data reduction procedure, and an uncertainty estimated can be derived. Finally, it is shown that 0.9997 ± 0.0003 is a nominal value for the internal quantum efficiency of one type of photodiode over the 440- to 460-nm spectral region.
[Contact: Jon Geist, (301) 975-2066]

Geist, J., Robinson, A.M., and James, C.R., **Numerical Modeling of Silicon Photodiodes for High-Accuracy Applications. Part III: Interpolating and Extrapolating Internal Quantum-Efficiency Calibrations**, Journal of Research of the National Institute of Standards and Technology, Vol. 96, No. 4, pp. 481-492 (July-August 1991).

The semiconductor device modeling program PC-1D and the programs that support its use in high-accuracy modeling of photodiodes, all of which were described in Part I, are used to simulate the interpolation of high-accuracy internal quantum-efficiency calibrations near 450 nm and 850 nm to the spectral region between these wavelengths. Convenient interpolation formulae that depend only upon wavelength are derived, as are uncertainty spectra for a number of sources of error. The formulae are normalized to experimental internal quantum-efficiency calibrations in the 440- to 470-nm spectral region and at 860 nm, and used to interpolate the calibrations to intermediate wavelengths. The results of the interpolations are compared with experimental calibration data that are available at a few wavelengths between 440 and 860 nm. The disagreement between the interpolated and measured internal quantum-efficiency data is never worse than 0.0003.
[Contact: Jon Geist, (301) 975-2066]

Seiler, D.G., Harman, G.G., Lowney, J.R., Mayo, S., and Liggett, W.S., Jr., **HgCdTe Detector Reliability Study for the GOES Program**, NISTIR 4687 (September 1991).

This report summarizes the results of a special assessment carried out by the National Institute of Standards and Technology (NIST) at the request of the National Oceanic and Atmospheric Administration of the reliability of certain infrared detectors for the Geostationary Operational Environmental Satellite (GOES) system. The data made available by ITT on detector resistances and signals support the conclusion that degradation of some detector responses has occurred, even when the estimated measurement uncertainty is included. Statistical analysis of the 11-μm detectors confirmed that detector 11-105 decreased in signal with time. The existing data available to NIST are not sufficient to identify uniquely the cause of degradation or unstable behavior present in a number of detectors. NIST's physical examination of several detectors by optical and SEM microscopy methods and an examination and analysis of a detector measurement database has yielded several plausible possible mechanisms for the observed degradation. These possible mechanisms are related to the detector fabrication or processing steps and include: incomplete or poor passivation procedures, excess mercury diffusion resulting from the ion-beam milling fabrication step, poor indium electrical contacts produced by the indium-plated fabrication step, and delamination of the ZnS anti-reflection optical coating. Other observed problems were poor wire bonding, use of tin-lead solder to couple the fine gold

wire (bonded to the detector) to the package terminal, and use of silicone RTV to stake the bond wires to the edge of the ZnS substrate.
[Contact: David G. Seiler, (301) 975-2081]

Radiation Effects

Released for Publication

Witczak, S.C., Suehle, J.S., Gaitan, M., and Yang, C.H., **An Experimental Comparison of Measurement Techniques to Extract Si-SiO_2 Interface Trap Density.**

For the first time, five methods of measuring Si-SiO_2 interface trap densities were compared on three otherwise identical MOSFETs which were radiation-stressed so as to induce different levels of interface trap densities. The results show that when sources of error and limitations are taken into account, these methods capable of estimating interface trap densities are in good quantitative agreement. Furthermore, the change in measured interface trap densities with radiation is independent of the method used. A comprehensive review of the methods is presented.
[Contact: John S. Suehle, (301) 975-2243]

Reliability

Released for Publication

Schafft, H.A., and Suehle, J.S., **The Measurement, Use, and Interpretation of the Temperature Coefficient of Resistance of Metallizations.**

The accurate measurement of the temperature coefficient of resistance (TCR) of thin-film, aluminum-based interconnects has many important applications for the reliability of microelectronics. The TCR is used to determine the metallization temperature in electromigration accelerated stress tests, a key element in characterizing the metallization. It can be used as a monitor for metal impurities and changes in structure that may have an impact on the reliability of the metal film. The resistance-versus-temperature behavior can be used to detect process variations that result in changes in cross-sectional areas of interconnect lines and residual resistivity. Also, the TCR permits metal lines to be used as temperature sensors that provide useful data for characterizing thermal environments and for thermal modeling that, again, impact reliability.

To permit the effective use of TCR for these applications, this paper describes the measurement, use, and interpretation of the temperature dependence of thin-film interconnects in ways that will help avoid many pitfalls and problems involved in the measurement and use of TCR. This paper is also intended to complement the JEDEC Standard in preparation on the temperature coefficient of resistance of metallization lines.
[Contact: Harry A. Schafft, (301) 975-2234]

Other Semiconductor Metrology Topics

Recently Published

Cummings, C.K., **Office of Microelectronics Programs Opens at NIST**, SRC Newsletter, Vol. 9, No. 9, pp. 3-4 (September 1991).

The Office of Microelectronic Programs has been established, with Robert I. Scace as Director, in the NIST Electronics and Electrical Engineering Laboratory. The responsibility of the Office is to coordinate important semiconductor measurement problems in industry with technical and scientific skills available in NIST. The purpose and function of the Office are briefly discussed, and examples of programs being carried out under the Office are identified.
[Contact: Carol K. Cummings, (301) 975-3075]

Scace, R.I., **Metrology for the Semiconductor Industry**, NISTIR 4653 (September 1991).

This report reviews the metrological needs of the semiconductor industry and its infrastructure, the materials and equipment industries that supply it, for the remainder of the present decade to the extent that they now can be foreseen. The text will also appear as one chapter of a larger assessment of needs for the electronics industry to be published later in 1991.

Only a needs assessment is included here. The manner in which the needs can be met is not discussed, largely because the task is of such a magnitude that no single organization can possibly do the necessary research and development on the time scale that the industry requires. Clearly, there is ample oppor-

tunity for contributions from universities, industrial laboratories, and government organizations such as NIST.

One principal purpose for preparing this report is to guide the planning of NIST's activities. Identification of the needs is only the first step in planning. Priorities must also be set. These depend on feedback from the industries that need the measurements described here, on knowledge of the work of others who may be working on related topics, and on the resources available to NIST. So much must be done that the luxury of duplicated efforts cannot be afforded.

This report draws on numerous recent publications of workshops and technology forecasts that are footnoted in the text. Early drafts were reviewed by others in the industry whose comments and advice are gratefully acknowledged.
[Contact: Robert I. Scace, (301) 975-2220]

SIGNAL ACQUISITION, PROCESSING, AND TRANSMISSION

DC and Low-Frequency Metrology

Recently Published

Burroughs, C.J., and Hamilton, C.A., **Voltage Calibration Systems Using Josephson Junction Arrays,** IEEE Transactions on Instrumentation and Measurement, Vol. 39, No. 6, pp. 972-975 (December 1990).

The recent development of large arrays of Josephson junctions is allowing an ever-increasing number of laboratories to maintain intrinsic Josephson voltage standards at an accuracy level near 0.05 parts per million. This paper reviews the fundamentals of Josephson voltage standards and shows how computer control makes these standards simple to use in a variety of applications.
[Contact: Charles J. Burroughs, (303) 497-3901]

Waveform Metrology

Released for Publication

Chesnut, S.M., and Paulter, N.G., **AWAMS User Manual,** to be published as NISTIR 3978.

The theory and operation of an upgraded version of the National Institute of Standards and Technology (NIST) Automatic Waveform Analysis and Measurement System (AWAMS) is described. This system was commissioned by the Army Primary Standards Laboratory to facilitate measurement comparability with NIST. The AWAMS has been installed at Redstone Arsenal, Alabama.
[Contact: S. Michelle Chesnut, (303) 497-3456]

Oldham, N.M., Hetrick, P.S., Kramar, J., Penzes, W., Wheatley, T., and Teague, C., **Electronic Limitations in Phase Meters for Heterodyne Interferometry,** to be published in the Proceedings of the Sixth Annual Conference of the American Society for Precision Engineering, Santa Fe, New Mexico, October 16, 1991.

Reasonable attention has been given to the fidelity of the process by which heterodyne interferometers convert optical path difference between beams that have traversed a test leg and a reference leg, respectively, to a phase difference between electrical signals from the reference and test photodetectors. This paper reports on a study of the next step: to obtain a quantitative result from these signals by measuring the electrical phase difference between the two photodetector signals.
[Contact: Nile M. Oldham, (301) 975-2408]

Paulter, N.G., Jr., and Stafford, R.B., **Minimizing the Effects of Record Truncation Discontinuities in Waveform Deconvolutions.**

We examine the results of waveform deconvolutions in which the waveforms have been modified to minimize the effects of record truncation discontinuities. Expressions describing the Fourier transform of these techniques are derived and verified by computer simulation. An analysis of the errors is given for each case.
[Contact: Nicholas G. Paulter, Jr., (303) 497-3400]

Recently Published

Oldham, N.M., and Hetrick, P.S., **High-Frequency, High-Speed Phase-Angle Measurements and Standards,** Proceedings of the 1991 National Conference of Standards Laboratories Workshop and Symposium, Albuquerque, New Mexico, August 18-22, 1991, pp. 251-256 (August 1991).

Counter-timers capable of measuring the delay between two signals at frequencies up to 20 MHz have been evaluated as phase angle meters with applications in heterodyne interferometry. A scheme for calibrating these instruments, both statically and dynamically (with the phase angle changing as fast 10°/μs), is described.
[Contact: Nile M. Oldham, (301) 975-2408]

Cryoelectronic Metrology

Released for Publication

Hamilton, C.A., and Gilbert, K.C., **Margins and Yield in Single Flux Quantum Logic.**

Simulations are used to optimize the design of simple rapid-single-flux quantum (RSFQ) logic gates and to determine their margins. Optimizations based on maximizing the smallest (critical) margin result in critical margin values in the range 18 to 50%. A Monte Carlo approach is used to illustrate the relationship between margins and process yield. Based on single gate results, the results show that one sigma parameter spreads of less than about ±5% will be required to make medium- or large-scale integrated RSFQ logic circuits. Finally, a single-bit full adder using five RSFQ gates and a local self-timing network is simulated at the discrete component level. The full adder used 2000 A/cm^2 junctions with a specific capacitance of 0.04 pF/μm^2 and had a logic delay of 87 pS and a worst-case margin of ±10%. These results show that margin calculations on individual gates are not necessarily representative of the performance of these gates in complex networks.
[Contact: Clark A. Hamilton, (303) 497-3740]

Recently Published

Benz, S.P., and Burroughs, C.J., **Coherent Emission From Two-Dimensional Josephson Junction Arrays**, Applied Physics Letter, Vol. 58, No. 19, pp. 2162-2164 (13 May 1991).

Coherent emission has been generated by two-dimensional arrays of superconductor-insulator-superconductor Josephson junctions and detected in a junction coupled to the array through a dc-blocking capacitor. The detector junction exhibits Shapiro steps at frequencies corresponding to the voltage across single array junctions and ranging from 60 to 210 GHz. The maximum power coupled to the detector junction occurs at 150 GHz and is estimated to be 0.4 μW, based on simulations of the detector circuit. Possible mechanisms for coherent emission from two-dimensional arrays are discussed.
[Contact: Sam P. Benz, (303) 497-3988]

Burroughs, C.J., and Hamilton, C.A., **Voltage Calibration Systems Using Josephson Junction Arrays**, IEEE Transactions on Instrumentation and Measurement, Vol. 39, No. 6, pp. 972-975 (December 1990).

The recent development of large arrays of Josephson junctions is allowing an ever-increasing number of laboratories to maintain intrinsic Josephson voltage standards at an accuracy level near 0.05 parts per million. This paper reviews the fundamentals of Josephson voltage standards and shows how computer control makes these standards simple to use in a variety of applications.
[Contact: Charles J. Burroughs, (303) 497-3901]

Grossman, E.N., McDonald, D.G., and Sauvageau, J.E., **Two-Dimensional Analysis of Microbolometer Arrays**, Journal of Applied Physics, Vol. 68, No. 11, pp. 5409-5414 (1 December 1990).

A two-dimensional, time-dependent analysis is made of array-compatible bolometers directly deposited onto a single substrate. It applies both to antenna-coupled and surface-absorbing configurations. Unlike previous spherically symmetric treatments, it allows analysis of thermal crosstalk between closely neighboring detectors and of the effects of finite substrate thickness. It is shown that in a closely packed array of surface-absorbing detectors, thermal crosstalk generally degrades the array's resolution more severely than optical (diffractive) crosstalk. Diffraction-limited resolution with surface-absorbing detectors is only possible by sacrificing either thermal resistance, and therefore sensitivity, or filling factor. With a minimum substrate thickness of L_{min}, a closely packed, diffraction-limited array is limited to a thermal resistance of $Z, \leq 0.08(\kappa L_{min})^{-1}$, where κ is the thermal conductivity of the substrate. An array of antenna-coupled bolometers is not subject to this limitation since the thermally and optically sensitive

areas need not be equal.
[Contact: E. N. Grossman, (303) 497-5102]

Antenna Metrology

Released for Publication

Repjar, A.G., Kremer, D.P., Guerrieri, J.R., and Canales, N., **Determining Faults on a Flat Phased Array Antenna Using Planar Near-Field Techniques,** to be published in the Proceedings of the Antenna Measurements Technique Association Conference, Boulder, Colorado, October 7-11, 1991.

The Antenna Metrology Group of the National Institute of Standards and Technology (NIST) has recently developed and implemented measurement procedures to diagnose faults on a flat phased-array antenna. First, the antenna was measured on the NIST planar near-field (PNF) range, taking measurements on a plane where the multiple reflections between the probe and the antenna under test are minimized. This is important since the PNF method does not directly allow for their effects. Then, the NIST PNF software which incorporates the fast Fourier transform (FFT) was used to determine the antenna's gain and pattern, and to evaluate the antenna's performance. Next, the inverse FFT was used to calculate the fields at the aperture plane. By using this technique, errors in the aperture fields due to multiple reflections can be avoided. By analyzing these aperture plane data through the use of detailed amplitude and phase contour plots, faults in the antenna were located and corrected. The PNF theory and utilization of the inverse FFT is briefly discussed and results are shown.
[Contact: Andrew G. Repjar, (303) 497-5703]

Recently Published

Muth, L.A., **Analytic Correction for Probe-Position Errors in Spherical Near-Field Measurements** [original title: An Analytic Technique to Correct Probe-Position Errors in Spherical Near-Field Measurements], Proceedings of the Seventh International Conference on Antennas and Propagation, York, United Kingdom, April 15-18, 1991, pp. 762-765 (1991).

A recently developed analytic technique that can correct for probe position errors in planar near-field measurements to arbitrary accuracy is shown to be also applicable to spherical near-field data after appropriate modifications. The method has been used successfully to remove probe position errors in the planar near field, leading to more accurate far-field patterns, even if the maximum error in the probe's position is as large as 0.2 λ. Only the error-contaminated near-field measurements and an accurate probe position error function are needed to be able to implement the correction technique. It is assumed that the probe position error function is a characteristic of the near-field range, and that it has been obtained using state-of-the-art laser positioning and precision optical systems. The method also requires the ability to obtain derivatives of the error-contaminated near field defined on an error-free regular grind with respect to the coordinates. In planar geometry the derivatives are obtained using FFTs, and in spherical geometry one needs to compute derivatives of Hankel functions for radial errors and derivatives of the spherical electric and magnetic vector basis functions for errors in the θ and ϕ coordinates. Efficient computer codes have been developed to accomplish this.
[Contact: Lorant A. Muth, (303) 497-3603]

Muth, L.A., **General Analytic Correction for Probe-Position Errors in Spherical Near-Field Measurements,** Journal of Research of the National Institute of Standards and Technology, Vol. 96, No. 4, pp. 391-410 (July-August 1991).

A general theoretical procedure is presented to remove known probe-position errors in spherical near-field data to obtain highly accurate far fields. We represent the measured data as a Taylor series in terms of the displacement error and the ideal spectrum of the antenna. This representation is then assumed to be an actual near field on a regularly spaced error-free spherical grid. The ideal spectrum is given by an infinite series of an error operator acting on data containing errors of measurement. This error operator is the Taylor series without the zeroth-order term. The nth-order approximation to the ideal near field of the antenna can be explicitly constructed by inspection of the error operator. Computer simulations using periodic error functions show that we are dealing with a convergent series, and the error-correction technique is highly successful. This is demonstrated for a triply periodic function for errors in each of the spherical coordinates. Appropri-

ate graphical representations of the error-contaminated, error-corrected, and error-free near fields are presented to enhance understanding of the results. Corresponding error-contaminated and error-free far fields are also obtained.
[Contact: Lorant A. Muth, (303) 497-3603]

Muth, L.A., and Lewis, R.L., **Personal Computer Codes for Analysis of Planar Near Fields,** NISTIR 3970 (June 1991).

We have developed FORTRAN codes for analysis of planar near-field data. We describe some of the inner workings of the codes, the data management schemes, and the structure of the input/output sections to enable scientists and programmers to use these codes effectively as a research tool in antenna metrology. The open structure of the codes allows a user to incorporate into the package new applications for future use with relative ease. The subroutines currently in existence are briefly described, and a table showing the interdependence among these subroutines is constructed. Some basic research problems, such as transformation of a near field to the far field and correction of probe position errors, are carried out from start to finish to illustrate use and effectiveness of these codes. Sample outputs are shown. The advantage of a high degree of modularization is demonstrated by the use of DOS batch flies to execute FORTRAN modules in a desired sequence.
[Contact: Lorant A. Muth, (303) 497-3603]

Microwave and Millimeter-Wave Metrology

Released for Publication

Daywitt, W.C., and Billinger, R.L., **A Simple Method for Measuring Adapter Efficiency.**

A swept frequency technique is presented that measures adapter efficiency across a given frequency band.
[Contact: William C. Daywitt, (303) 497-3720]

Williams, D.F., **Monolithic Microwave Integrated Circuit Metrology.**

The metrology of monolithic microwave integrated circuits is discussed. The relevance of transmission lines and their probes to the required measurements is explored.
[Contact: Dylan F. Williams, (303) 497-3138]

Williams, D.F., **NIST Consortium Develops Microwave Standards for MMIC Measurements.**

As the manufacturing costs of monolithic microwave integrated circuits (MMICs) have decreased, testing costs have become an increasingly significant proportion of total circuit cost. This has stimulated a revolution in the way in which MMICs are tested. Standards and calibration techniques developed for these measurements by the NIST Industrial MMIC Consortium are discussed.
[Contact: Dylan F. Williams, (303) 497-3138]

Recently Published

Daywitt, W.C., **Exact Principal Mode Field for a Lossy Coaxial Line,** IEEE Transactions on Microwave Theory and Techniques, Vol. 39, No. 8, pp. 1313-1322 (August 1991).

Exact field equations for a lossy coaxial transmission line with an infinite outer conductor are presented. The corresponding determinantal equation is solved to obtain an exact propagation constant from which errors in the microwave approximation and an alternative full frequency range approximation are calculated. The calculations show that the microwave approximation, although containing a large relative error at the lower frequencies, is still useful in practical applications.
[Contact: William D. Daywitt, (303) 497-3720]

Marks, R.B., **A Multiline Method of Network Analyzer Calibration,** IEEE Transactions on Microwave Theory and Techniques, Vol. 39, No. 7, pp. 1205-1215 (July 1991).

This paper presents a new method for the calibration of network analyzers. The essential feature is to use the multiple, redundant transmission line standards. The additional information provided by the redundant standards is used to minimize the effects of random errors, such as those due to imperfect connector repeatability. The resulting method exhibits improvements in both accuracy and bandwidth over conventional methods. The basis of the statistical treatment is a linearized error analysis of the through-reflect-line calibration method. This analysis, presented here, is

useful in the assessment of calibration accuracy. It also yields new results relevant to the choice of standards.
[Contact: Roger B. Marks, (303) 497-3037]

Williams, D.F., and Marks, R.B., **Transmission Line Capacitance Measurement** [original title: Approximate Determination of the Capacitance of Coplanar Lines], IEEE Microwave and Guided Wave Letters, Vol. 1, No. 9, pp. 243-245 (September 1991).

The capacitance and conductance per unit length of a transmission line are useful in the determination of its characteristic impedance, particularly with lossy transmission lines such as coplanar waveguide. The capacitance of coplanar lines is measured with two independent techniques. The results of both measurements agree closely with calculations. A technique for directly comparing the capacitance of two similar transmission lines is also demonstrated.
[Contact: Dylan F. Williams, (303) 497-3138]

Electromagnetic Properties

Released for Publication

Baker-Jarvis, J.R., Geyer, R.G., and Domich, P.D., **A Nonlinear Regression Technique for Transmission Line Permittivity and Permeability Determination.**

A technique for the solution of one-port and two-port scattering equations for complex permittivity and permeability determination is presented. Using a nonlinear regression procedure, the model determines parameters for the specification of the spectral functional form of complex permittivity and permeability. The method is based on the fact that a causal, analytic function can be represented by pole and zero data. The technique allows the accurate determination of many low- and high-permittivity dielectric or magnetic materials in either the low- or high-loss range. It has been found that permeability and permittivity can be obtained either from fitting all scattering parameter data or by fitting S_{21}, or S_{11} data or $|S_{11}|$ and $|S_{21}|$ data. The model allows for small adjustments to independent variable data such as angular frequency, sample length, sample position, and cutoff wavelength, consistent with the physics of the problem. The model can determine permittivity and permeability for samples where sample length, sample position, and sample holder length are not known precisely.
[Contact: James R. Baker-Jarvis, (303) 497-5621]

Gans, W.L., Geyer, R.G., and Klemperer, W.K., **Quantifying Standard Performance of Electromagnetic-Based Mine Detectors,** to be published as NISTIR 3982.

This is a final report to the sponsor on work performed by National Institute of Standards and Technology (NIST) personnel from January 1, 1985 to December 31, 1990. An overview of the theory of the electromagnetic (EM) properties of soils is presented, along with a brief review of existing technologies for the detection of buried objects using electromagnetics. The critical electromagnetic performance factors for portable EM mine detectors that NIST has identified are presented, along with a discussion of measurement systems for measuring the constitutive properties of soil and mine-like materials. Recommendations are then presented for a measurement system configuration that should meet most of the Army's requirements. A recommended mine detector testing strategy is then presented along with a set of instructions for specific tests and an algorithm for comparatively scoring the performance of detectors. The tests and the scoring algorithm are as specific and as detailed as is possible at this stage of development. Last, a section is included that contains NIST's recommendations for the test data that should be archived.
[Contact: William L. Gans, (303) 497-3538]

Tofani, S., Ondrejka, A.R., Kanda, M., and Hill, D.A, **Bistatic Scattering of Absorbing Materials From 30 to 1000 MHz.**

A wideband time-domain reflectometer has been used to evaluate the bistatic performance of the scattering coefficient of rf/microwave absorbers. The scattering coefficient has been measured inside an anechoic chamber in the 30- to 1000-MHz frequency range in the case of specular reflection. The scattering coefficient increases with incidence angle, and the measurement accuracy is ±2 dB.
[Contact: Arthur R. Ondrejka, (303) 497-3309]

Recently Published

Tofani, S., Ondrejka, A.R., and Kanda, M., **A Time-Domain Method for Characterizing the Reflection Coefficient of Absorbing Materials from 30 to 1000**

MHz [original title: Time-Domain Method for Absorbing Material Reflectivity Characterization in the 30-1000 MHz Frequency Range], IEEE Transactions on Electromagnetic Compatibility, Vol. 33, No. 3, pp. 234-240 (August 1991).

A wideband time-domain reflectometer is used to evaluate the reflection characteristics of rf/microwave absorbers. The reflectometer uses an array of two identical broadband antennas, both transmitting and receiving. The method uses the two antennas in a difference mode to remove the undesired signals and to enhance the small reflections being measured. Using this technique, we can separate front surface reflections from those which are generated at greater angles. The spectrum bandwidth of our pulses is 30 MHz to 1000 MHz, and reflection characteristics are measured over this entire range. The method has been used to characterize the reflectivity of three different types of absorber placed in an anechoic chamber. The results are reported together with the measurement accuracy. A discussion regarding main sources of errors is also presented.
[Contact: Arthur R. Ondrejka, (303) 497-3309]

Laser Metrology

Recently Published

Scott, T.R., **Megawatt Laser Calorimeter Design**, Conference Record, IEEE Instrumentation and Measurement Technology Conference, Atlanta, Georgia, May 14-16, 1991, pp. 227-231 (1991).

The accurate determination of laser energy becomes extremely difficult when seeking to measure the output of laser sources having average powers in the megawatt range. This paper describes the conceptual design of a calorimeter which could safely capture the output of megawatt-class, continuous-wave laser sources operating in the near-infrared wavelength region. A primary consideration in this design was the possibility that at some point in the future it would have to be scaled to even larger dimensions. Accordingly, the design uses non-exotic optical techniques and a simple geometry to handle the high power densities expected from the laser sources. An array of curved, reflective rods is used to spread the laser radiation before it is absorbed by a black-walled cavity. The calorimeter is designed to capture the entire laser beam with subsequent conversion of the electromagnetic energy to thermal energy. The temperature of the calorimeter is monitored and used to determine the incident laser radiation.
[Contact: Thomas R. Scott, (303) 497-3651]

Optical Fiber Metrology

Released for Publication

Danielson B.L., **Precision Length Measurements in Multimode Optical Fibers.**

By using selective optical excitation, both the group index and group delay of on-axis modes of multimode fibers can be determined with high precision. The group index of several types of fibers was measured at 1310 nm in a fiber Michelson interferometer, and the values tabulated. Group delays were obtained from the transit time of short duration optical pulses. From these data, the length of reference fibers about 2 km long was calculated. Length measurement accuracy was limited by group index uncertainties to about 0.04%. Also, a technique is described which uses these reference fibers to minimize uncertainties in distance measurements made with multimode optical time domain reflectometers.
[Contact: Bruce L. Danielson, (303) 497-5620]

Mamileti, L., Wang, C.M., Young, M., and Vecchia, D.F., **Optical Fiber Geometry by Gray Scale Analysis with Robust Regression.**

We have used least-median-of-squares (LMS) regression to analyze gray-scale images of optical fiber ends. LMS regression is a form of robust regression and ignores outlying data points. We fitted the images of each of two fiber ends to an ellipse by LMS and least-sum-of-squares regression. The two methods yielded nearly identical results on a pristine fiber end, but the LMS method was far superior on a damaged fiber end, even though we made no effort to filter the outlying data points.
[Contact: Matt Young, (303) 497-3223]

Recently Published

Franzen, D.L., **Precision Measurements on Optical Fibers**, Optics & Photonics News, pp. 30-31 (May 1991).

The precision and accuracy of single-mode optical fiber measurements are discussed. Included in the discussion are measurements for: attenuation, mode-field diameter, cut-off wavelength, and geometrical parameters.
[Contact: Douglas L. Franzen, (303) 497-3346]

Young, M., **Fiber Cladding Diameter by Contact Micrometry**, Conference Digest, Optical Fibre Measurement Conference, York, United Kingdom, September 17-18, 1991, pp. 123-126 (1991).

This paper reports very precise measurements of the cladding diameter of optical fibers by contact micrometry. A committee of the Telecommunications Industry Association was reluctant to accept an artifact standard other than an optical fiber because the measured result is a function of illumination, and because reflection from a metal film displays phase shifts that are not present in reflection from a glass edge. Indeed, the concern about phase shifts is not misplaced; we have measured widths of chrome-on-glass lines with a scanning confocal microscope and found the measured results to change by nearly 0.1 μm with polarization. At any rate, even if a chrome-on-glass standard is finally adopted, it is necessary to measure a fiber very accurately to verify the relevance of the chrome standard.
[Contact: Matt Young, (303) 497-3223]

Optical Fiber Sensors

Released for Publication

Patterson, R.L., Rose, A.H., Tang, D., and Day, G.W., **Fiber-Optic Sensors for Aerospace Electrical Measurements: An Update**, to be published as a NASA Technical Memorandum. [Also to be published in the Proceedings of the 26th Intersociety Energy Conversion Engineering Conference, IECEC-91, Boston, Massachusetts, August 4-9, 1991.]

Fiber-optic sensors are being developed for electrical current, voltage, and power measurements in aerospace applications. These sensors are presently designed to cover ac frequencies from 60 Hz to 20 kHz. The current sensor, based on the Faraday effect in optical fiber, is in advanced development after some initial testing. Concentration is on packaging methods and ways to maintain consistent sensitivity with changes in temperature. The voltage sensor, utilizing the Pockels effect in a crystal, has excelled in temperature tests. This paper reports on the development of these sensors. It also relates the technology used in the sensors, the results of evaluation, improvements now in progress, and the future direction of the work.
[Contact: Allen H. Rose, (303) 497-5599]

Rose, A.H., and Day, G.W., **Optical Fiber Voltage Sensors for Broad Temperature Ranges**, to be published in the Proceedings of SPIE (The International Society for Optical Engineering, P.O. Box 10, Bellingham, Washington 98227-0010), Fiber Optic Components & Reliability, Boston, Massachusetts, September 3-6, 1991.

In this paper, we describe the development of an optical fiber ac voltage sensor for aircraft and spacecraft applications. Among the most difficult specifications to meet for this application is a temperature stability of ±1% from -65 °C to +125 °C. This stability requires a careful selection of materials, components, and optical configuration with further compensation using an optical fiber temperature sensor located near the sensing element. The sensor is a polarimetric design, based on the linear electro-optic effect in bulk bismuth germanate ($Bi_4Ge_3O_{12}$). The temperature sensor is also polarimetric, based on the temperature dependence of the birefringence of bulk SiO_2. The temperature sensor output is used to automatically adjust the calibration of the instruments.
[Contact: Allen H. Rose, (303) 497-5599]

Rose, A.H., Deeter, M.N., and Day, G.W., **High Sensitivity, High Speed Current Sensor Based on the Faraday Effect in Ga:YIG**, to be published in the Proceedings of the Eighth Optical Fiber Sensors Conference, Monterey, California, January 27-31, 1992.

We demonstrate an optical fiber current sensor based on the Faraday effect in gallium-doped yttrium iron garnet that has a measured sensitivity of approximately 3.1 °/A, a noise equivalent current of about 14 μA/✓Hz, and 3-dB bandwidth of approximately 10 MHz. The sensitivity-bandwidth product is about a factor of 600 greater than previously achievable.
[Contact: Allen H. Rose, (303) 497-5599]

Wolfe, R., Gyorgy, E.M., Lieberman, R.A., Fratello,

V.J., Licht, S.J., Deeter, M.N., and Day, G.W., **High Frequency Magnetic Field Sensors Based on the Faraday Effect in Garnet Thick Films**, to be published in the Proceedings of the Eighth Optical Fiber Sensors Conference, Monterey, California, January 29-31, 1992.

Thick films of modified yttrium iron garnet with uniaxial magnetic anisotropy can be used in fiber optic magnetic-field sensors. Theory and experiments show good sensitivity and upper frequency limits between 10^6 and 10^9 Hz.
[Contact: Merritt N. Deeter, (303) 497-5400]

Recently Published

Deeter, M.N., Rose, A.H., and Day, G.W., **Faraday-Effect Magnetic Field Sensors Based on Substituted Iron Garnets**, Proceedings of SPIE (The International Society for Optical Engineering, P.O. Box 10, Bellingham, Washington 98227-0010), Fiber Optic and Laser Sensors VIII, San Jose, California, September 16-21, 1990, pp. 243-245 (1990).

The performance of fiber-optic magnetic field sensors based on the Faraday effect mainly depends on the magneto-optic properties of the sensor element. Certain ferrimagnetic materials known as substituted iron garnets display characteristics which make them suitable for applications of magnetometry requiring high sensitivity, high spatial resolution, or high speed. The potential of these materials for magnetic field sensing is illustrated by comparing results of measurements made on two different iron garnet compositions.
[Contact: Merritt Deeter, (303) 497-5400]

Tang, D., Rose, A.H., Day, G.W., and Etzel, S.M., **Annealing of Linear Birefringence in Single-Mode Fiber Coils: Application to Optical Fiber Current Sensors**, Journal of Lightwave Technology, Vol. 9, No. 8, pp. 1031-1037 (August 1991).

Annealing procedures that greatly reduce linear birefringence in single-mode fiber coils are described in detail. These procedures have been successfully applied to coils ranging from 5 mm to 10 cm in diameter and up to 200 or more turns. They involve temperature cycles that last 3 to 4 days and reach maximum temperatures of about 850 °C. The primary application of these coils is optical fiber current sensors, where they yield small sensors that are more stable than those achieved by other techniques. A current sensor with a temperature stability of $+8.4 \times 10^{-5}$/K over the range from -75 to +145 °C has been demonstrated. This is approximately 20% greater than the temperature dependence of the Verdet constant. Packaging degrades the stability, but a packaged sensor coil with a temperature stability of about $+1.6 \times 10^{-4}$/K over the range from -20 to +120 °C has also been demonstrated.
[Contact: Allen H. Rose, (303) 497-5599]

Williams, P.A., Day, G.W., and Rose, A.H., **Compensation for the Temperature Dependence of Faraday Effect in Diamagnetic Materials: Application to Optical Fiber Sensors**, Electronics Letters, Vol. 27, No. 13, pp. 1131-1132 (20 June 1991).

The temperature dependence of the Faraday effect in a diamagnetic material can be compensated by varying the polarization state of the light entering the material as a function of temperature. We demonstrate that this can be done automatically by exploiting the temperature dependence of a linear retarder (waveplate).
[Contact: Paul Williams, (303) 497-3287]

Electro-Optic Metrology

Released for Publication

Esman, R.D., and Iwashita, I., **High-Frequency Optical FM Noise Reduction Employing a Fiber-Insertable Feedforward Compensation Technique**, to be published in Optical Fiber Conference '92, San Jose, California, February 3-7, 1992.

High-frequency (~1 GHz) optical phase noise, as sampled by a Mach-Zehnder frequency discriminator with an integrating receiver, is fedforward (out-of-phase) to a subsequent phase modulator. The canceling technique results in linewidth and phase noise reduction.
[Contact: Aaron A. Sanders, (303) 497-5341]

Gilbert, S.L., **High Resolution Spectroscopy Using Fiber Lasers**, to be published in the Proceedings of the Tenth International Conference on Laser Spectroscopy, Font-Romev, France, June 17-21, 1991.

Fiber lasers show potential for use in high-resolution laser spectroscopy. Tunable, single-longitudinal-mode operation has been achieved with free-running laser linewidths of about 1 MHz. It would be straightforward to obtain much narrower linewidths using low-frequency electronic feedback. In this paper, I review this rapidly changing field and discuss the use of fiber lasers in spectroscopy.
[Contact: Sarah L. Gilbert (303) 497-3120]

Obarski, G.E., **Lambdameter for Accurate Stability Measurements of Optical Transmitters,** to be published in the Proceedings of SPIE (The International Society for Optical Engineering, P.O. Box 10, Bellingham, Washington 98227-0010), Laser Testing and Reliability, San Jose, California, November 3-8, 1991.

Very wavelength-stable, single-mode laser diodes will play an important role in near-future optical fiber communications systems. Two such applications are sources for dense wavelength multiplexing and local oscillators in coherent systems. To accurately measure wavelength of 1.3- and 1.5-μm single-mode sources, we developed a lambdameter that can also be used in the near IR and red regions of the spectrum. Wavelength accuracy and resolution are ≈0.1 parts per million at the 0.63-μm HeNe laser emission line. They were measured by comparing each of two adjacent modes of a HeNe laser, frequency-stabilized by a polarization technique, with a single mode from a second frequency-stabilized HeNe laser. We also verified the wavelength of the reference laser to 1 part-per-million accuracy by comparing it with the 1.52-μm HeNe laser emission line. The uncertainty in wavelength of the 1.52-μm HeNe laser is limited to the width of the Doppler gain curve whose peak is known within 0.2 parts per million. We describe our lambdameter and the performance of its reference laser as a wavelength transfer standard. Measurements on a commercially packaged 1.52-μm DFB-laser diode transmitter show that its wavelength fluctuates by at least 1 part per million during normal changes in room temperature.
[Contact: Gregory E. Obarski, (303) 497-5747]

Schlager, J.B., Kawanishi, S., and Saruwatari, M., **Dual Wavelength Pulse Generation Using a Mode-Locked Erbium-Doped Fiber Ring Laser.**

Dual pulses, each with durations as short as 2 ps and different peak wavelengths, were concurrently produced with an actively mode-locked, erbium-doped fiber ring laser made in part with birefringent polarization-maintaining fiber. Peak-wavelength separation was proportional to the percentage of cavity having properly aligned birefringent fiber.
[Contact: John B. Schlager, (303) 497-3542]

Recently Published

Deeter, M.N., Rose, A.H., and Day, G.W., **Fast, Sensitive Magnetic-Field Sensors Based on the Faraday Effect in YIG** [original title: High-Speed, High-Sensitivity Magnetic Field Sensors Based on the Faraday Effect in YIG], Journal of Lightwave Technology, Vol. 8, No. 12, pp. 1838-1842 (December 1990).

Magnetic field sensors based on the Faraday effect in ferrimagnetic iron garnets are characterized in terms of their sensitivity, speed, and directionality. Sensitivity measurements at 80 Hz on small (e.g., 5-mm-diameter by 3-mm-long) samples of yttrium iron garnet (YIG) yield noise equivalent magnetic fields of 10 nT/Hz. Frequency response measurements exhibit virtually flat response to approximately 700 MHz.
[Contact: Merritt N. Deeter, (303) 497-5400]

Tu, Y., Goyal, I.C., Gallawa, R.L., and Ghatak, A.K., **Optical Waveguide Modes: An Approximate Solution Using Galerkin's Method with Hermite-Gauss Basis Functions** [original title: Solving the Scalar Wave Equation: Expansion in Terms of Hermite Gauss Functions], IEEE Journal of Quantum Electronics, Vol. 27, No. 3, pp. 518-522 (March 1991).

In Galerkin's method, an orthogonal set of functions is used to convert a differential equation into a set of simultaneous linear equations. We choose the Hermite-Gauss functions as the set of orthogonal basis functions to solve the eigenvalue problem based on the two-dimensional scalar-wave equation subject to the radiation boundary conditions at infinity. The method gives an accurate prediction of modal propagation constant and of the field distribution. The method is tested by using the step-index optical fiber, which has a known exact solution, and the truncated parabolic profile fiber, for which trends are well known. We also test the method using square and elliptic core fibers. The method is found to agree

with known results.
[Contact: Robert L. Gallawa, (303) 497-3761]

Complex System Testing

Released for Publication

Stenbakken, G.N., and Souders, T.M., **Linear Error Modeling of Analog and Mixed-Signal Devices**, to be published in the Proceedings of the 1991 International Test Conference, Nashville, Tennessee, October-November 1, 1991.

Techniques are presented for developing linear error models for analog and mixed-signal devices. Methods for choosing parameters and assuring the models are complete and well-conditioned are included. Once established, the models can be used in a comprehensive approach for optimizing the testing of the subject devices.
[Contact: Gerard N. Stenbakken, (301) 975-2440]

Other Signal Topics

Released for Publication

Gans, W.L., Geyer, R.G., and Klemperer, W.K., **Quantifying Standard Performance of Electromagnetic-Based Mine Detectors,** to be published as NISTIR 3982.

This is a final report to the sponsor on work performed by National Institute of Standards and Technology (NIST) personnel from January 1, 1985 to December 31, 1990. An overview of the theory of the electromagnetic (EM) properties of soils is presented, along with a brief review of existing technologies for the detection of buried objects using electromagnetics. The critical electromagnetic performance factors for portable EM mine detectors that NIST has identified are presented, along with a discussion of measurement systems for measuring the constitutive properties of soil and mine-like materials. Recommendations are then presented for a measurement system configuration that should meet most of the Army's requirements. A recommended mine detector testing strategy is then presented along with a set of instructions for specific tests and an algorithm for comparatively scoring the performance of detectors. The tests and the scoring algorithm are as specific and as detailed as is possible at this stage of development. Last, a section is included that contains NIST's recommendations for the test data that should he archived.
[Contact: William L. Gans, (303) 497-3538]

Ma, M.T., and Adams, J.W., **Determination of Phase Characteristics and Time Responses of Unknown Linear Systems Based on Measured cw Amplitude Data**, to be published as NIST Technical Note 1349. [A condensed version, **System Response to Pulsed Excitations Estimated From Measurement of cw Amplitudes**, will be published in the Record of the 1992 International Symposium on Electromagnetic Compatibility, Beijing, China, May 25-27, 1992.]

An alternative technique is described for calculating the complete time and frequency characteristics of an unknown linear system from the measured amplitude response to continuous-wave (cw) excitations by assuming that the system transfer function is minimum phase. The time-response level so determined shows that the susceptibility of the system to damage by pulsed excitation is the greatest during the initial period of excitation. Other possible time responses, when the actual system transfer function is nonminimum phase, are also identified and analyzed.
[Contact: Mark T. Ma, (303) 497-3800]

Recently Published

Capobianco, T.E., and Ciciora, S.J., **Characterizing Differential Air-Core Eddy Current Probes**, Review of Progress in Quantitative Nondestructive Evaluation, Vol. 10A, D. O. Thompson and D. E. Chimenti, Eds. (Plenum Press, New York, 1991), pp. 897-903. [Proceedings of the Review of Progress in Quantitative Nondestructive Evaluation Conference, La Jolla, California, September 15-20, 1990.]

We report the results of measurements establishing the flaw response of a differential, air-core, eddy current probe. The parameters chosen for the probe's construction were picked from a set of 32 combinations of five factors which were varied at two levels. These five factors include: (1) the number of layers of the inner coils, (2) the number of layers of the outer coil, (3) the number of turns on the inner coils, (4) the number of turns on the outer coil, and (5) the inside diameter of the inner coils. We report the

results of calibrating this probe constructed in our laboratory, and we also discuss some of the idiosyncracies we encountered in the calibration process. The calibration reported here was carried out on seven notches made by electrical discharge machining in blocks of 7075-T6 aluminum alloy. The probe output is correlated to changes in flaw area.
[Contact: Thomas E. Capobianco, (303) 497-3141]

Field, B.F., and Fenimore, C., **Video Processing With the Princeton Engine at NIST**, NIST Technical Note 1288 (August 1991).

This document describes the NIST program in digital processing, including a newly created Image Processing Laboratory at NIST that is available to governmental, industrial, and academic researchers working on digital image processing. The centerpiece of the laboratory is a video supercomputer, the Princeton Engine, designed and constructed by the David Sarnoff Research Center. The engine provides real-time video and image-processing capability, accepting a variety of video formats over multiple wideband input channels and outputting real-time video for immediate viewing. Because the Engine is programmable, it is possible to use it to evaluate prototypes of image-processing components rapidly and efficiently.

The hardware capabilities of the Princeton Engine are described, as well as the available supporting video equipment in the Laboratory. Two programming examples are included to demonstrate the unusual programming environment and "language" used to program the Engine. Appendices list the available predefined library modules and the processor assembly language instructions.
[Contact: Bruce F. Field, (301) 975-4230]

Goyal, I.C., Gallawa, R.L., and Ghatak, A.K., **An Approximate Solution to the Wave Equation — Revisited** [original title: An Approximate Solution to Second Order Linear Homogeneous Differential Equations], Journal of Electromagnetic Waves and Applications, Vol. 5, No. 6, pp. 623-636 (1991).

We revisit here an old but neglected approximate analytic solution to the electromagnetic wave equation. Our method of derivation is reminiscent of the WKB methodology (WKB refers to the initials of three independent workers -- Wentzel, Kramers, Brillouin -- who first used the approximation procedure to solve the Schroedinger wave equation in one dimension), but the solution, although approximate, is much more accurate than the traditional WKB solution and can be used with almost as much ease. The method is extremely powerful but, to our knowledge, has never been used by the optics community, where its use in analyzing optical fibers and integrated optical waveguides would be beneficial.
[Contact: Robert L. Gallawa, (303) 497-3761]

ELECTRICAL SYSTEMS

Power Systems Metrology

Released for Publication

Martzloff, F.D., **IEEE Guide on Surge Voltages Upgraded to Recommended Practice.**

After ten years of use as a guide, a revision has been completed and published as an IEEE Recommended Practice: Surge Voltages in Low-Voltage AC Power Circuits. This is an article to be published in a trade magazine circulated to writers, users, and enforcers of standards on electromagnetic compatibility, in order to give them a preview of the forthcoming IEEE document.
[Contact: Francois D. Martzloff, (301) 975-2409]

Martzloff, F.D., and Lai, J.S., **Cascading Surge-Protective Devices: Coordination versus the IEC 664 Staircase**, to be published in the Proceedings of the First International Conference on Power Quality: End-Use Applications and Perspectives, Gif-sur-Yvette, Paris, France, October 15-18, 1991.

Cascading two or more surge-protective devices located, respectively, at the service entrance of a building and near the sensitive equipment is intended to ensure that each device shares the surge stress in a manner commensurate with its rating to achieve reliable protection of equipment against the surges impinging from the utility supply, as well as internally generated surges. However, depending upon the relative clamping voltages of the two devices, their separation distance, and the waveform of the impinging surge, coordination may or may not be effective. The paper reports computations confirmed by measurements of the energy deposited in the devices for combination of these three parameters.
[Contact: Francois D. Martzloff, (301) 975-2409]

Martzloff, F.D., and Mendes, A., **Standards: Transitional Aspects**, to be published in the Proceedings of the First International Conference on Power Quality: End-Use Applications and Perspectives, Gif-sur-Yvette, Paris, France, October 15-18, 1991.

Mass production of electrical and electronic equipment for the world market requires a system of standards of world-wide applicability. The development of such standards is a complex task, involving various national and international organizations. This paper presents a review of the standards-writing process, in particular, the area of power quality.
[Contact: Francois D. Martzloff, (301) 975-2409]

Misakian, M., **In Vitro Exposure Parameters with Linearly and Circularly Polarized ELF Magnetic Fields**, to be published as an abstract of Talk for 1991 DOE Contractors' Review, Milwaukee, Wisconsin, November 3-7, 1991.

A comparison is made of induced current densities, electric fields, and rate of energy deposition during in vitro studies with linearly and circularly polarized extremely low frequency (ELF) magnetic fields.
[Contact: Martin Misakian, (301) 975-2426]

Turgel, R.S., **Electricity in the Year 2000**, to be published in the Proceedings of the IEEE Technical Activities Board (TAB), Mexico City, Mexico, October 3, 1991.

Demand for electricity is predicted to rise at a rate higher than that of the creation of new generating capacity. Projections suggest that a shortfall of 100 million kilowatts may be reached by the year 2000. Various measures to alleviate the projected shortfall are discussed.
[Contact: Raymond S. Turgel, (301) 975-2420]

Van Brunt, R.J., **Discussion on Paper Entitled "Digital Techniques for Partial Discharge Measurement," A Report on the Activities of the Working Group on Digital Analysis of Partial Discharges**.

This is a brief discussion that points out inherent limitations to reliable and meaningful interpretation of data from phase-resolved measurements of partial-discharge pulse-height and phase-of-occurrence distributions currently being developed for investigation of aging phenomena in electrical insulation and for evaluation of insulation integrity. These limitations are due to memory propagation effects that cause the phenomenon to be susceptible to nonstationary behavior. It is pointed out that these limitations can be at least partly overcome by measuring various conditional partial-discharge pulse height and phase distributions.
[Contact: Richard J. Van Brunt, (301) 975-2425]

Recently Published

Martzloff, F.D., **On the Propagation of Old and New Surges**, Proceedings of the Open Forum on Surge Protection Application, Gaithersburg, Maryland, June 18-19, 1991, pp. 19-25 (1991).

The objective of the paper is to review the propagation characteristics of the old and new generation of surge waveforms encountered in low-voltage ac power systems. To complement information developed on this subject over the last ten years, measurement results are reported for the new 10/1000 μs waveform, and the effect (or, rather, the lack of effect) of wire size is documented by a simple experimental demonstration.
[Contact: Francois D. Martzloff, (301) 975-2409]

Martzloff, F.D., **Proceedings, Open Forum on Surge Protection Application**, Gaithersburg, Maryland, June 18-19, 1991, NISTIR 4657 (August 1991).

An Open Forum on Surge Protection Application was convened by the National Institute of Standards and Technology to provide a conduit for a wide range of positions, opinions, and needs to be fed into the voluntary standards-writing process. Twenty papers are included in the Proceedings, grouped in major categories of surge environment, device performance, application standards, installation practices, and coordination of cascaded devices. Appendices include a listing of the interests of the participants, their initial expectations, and an action wish list developed at the conclusion of the Forum.
[Contact: Francois D. Martzloff, (301) 975-2409]

Stricklett, K.L., Fenimore, C., Kelley, E.F., Yamashita, H., Pace, M.O., Blalock, T.V., Wintenberg, A.L., and Alexeff, I., **Observation of Partial Discharge in Hexane Under High Magnification,** IEEE Transactions on Electrical Insulation, Vol. 26, No. 4, pp. 692-698 (August 1991).

Partial discharges are observed in hexanes by shadow photography under the application of dc voltages. A nonuniform field geometry is employed, and the growth of cavities associated with partial discharges at a point cathode is photographed at 200X magnification. The use of an image-preserving optical delay allows a record of the conditions which exist in the liquid prior to the initiation of the partial discharge to be obtained; a simultaneous record of the partial discharge current is obtained. Analysis of these data indicates that electrostatic forces are adequate to drive streamer growth.
[Contact: Kenneth L. Stricklett, (301) 975-3955]

Van Brunt, R.J., Misakian, M., Kulkarni, S.V., and Lakdawala, V.K., **Influence of a Dielectric Barrier on the Stochastic Behavior of Trichel-Pulse Corona,** IEEE Transactions on Electrical Insulation, Vol. 26, No. 3, pp. 405-415 (June 1991).

The stochastic behavior of a negative, point-to-plane (Trichel-pulse) corona discharge in air has been investigated for the case where the plane electrode is partially covered with a solid PTFE (polytetrafluoroethylene) dielectric of varying size and position relative to the point electrode. This behavior is revealed from measurements of conditional and unconditional corona pulse-amplitude and pulse-time-separation distributions. The results indicate that the presence of a dielectric surface on the anode does not affect the occurrence of Trichel pulses provided the point-to-plane gap spacing is greater than a critical value d_c which depends on the size of the dielectric and the applied voltage. As the gap spacing approaches d_c, the effect of dielectric surface charging by the corona introduces measurable "memory effects" indicated by correlations between pulse amplitude and time separation from the previous pulse. For spacings less than d_c, detectable corona-pulse activity is quenched by the presence of a quasi-permanent surface charge on the dielectric.
[Contact: Richard J. Van Brunt, (301) 975-2425]

Magnetic Materials and Measurements

Released for Publication

Goldfarb, R.B., **Demagnetizing Factors.**

Demagnetizing factors for ellipsoids of revolution and right circular cylinders are reviewed.
[Contact: Ronald B. Goldfarb, (303) 497-3650]

Goldfarb, R.B., **Magnetic Measurements for High Energy Physics Applications,** to be published as NISTIR 3975.

This report is a collection of papers describing magnetic measurements on multifilamentary Nb-Ti superconductor wires and cables as a function of magnetic field and time at liquid-helium temperatures. The papers deal with ac losses and interfilament coupling by proximity effect and eddy currents. Flux creep was investigated under different experimental conditions. A Hall-probe magnetometer, which was used to measure magnetization and flux creep in the presence of a transport current, is described. A method for increasing the critical current of superconducting cable by controlling twist pitch is demonstrated. A critical-state model for the magnetization of superconductors was developed for samples with field-dependent critical-current density and rectangular cross section.
[Contact: Ronald B. Goldfarb, (303) 497-3650]

Recently Published

Deeter, M.N., Rose, A.H., and Day, G.W., **Faraday-Effect Magnetic Field Sensors Based on Substituted Iron Garnets,** Proceedings of SPIE (The International Society for Optical Engineering, P.O. Box 10, Bellingham, Washington 98227-0010), Fiber Optic and Laser Sensors VIII, San Jose, California, September 16-21, 1990, pp. 243-245 (1990).

The performance of fiber-optic magnetic field sensors based on the Faraday effect mainly depends on the magneto-optic properties of the sensor element. Certain ferrimagnetic materials known as substituted iron garnets display characteristics which make them suitable for applications of magnetometry requiring high sensitivity, high-spatial resolution, or high speed. The potential of these materials for magnetic field sensing is illustrated by comparing results of measure-

ments made on two different iron garnet compositions.
[Contact: Merritt N. Deeter, (303) 497-5400]

Moreland, J., and Rice, P., **Tunneling Stabilized, Magnetic Force Microscopy With a Gold-Coated, Nickel-Film Tip** [original title: Tunneling Stabilized, Magnetic Force Microscopy with a Au Coated, Ni-Film Tip], Journal of Applied Physics, Vol. 70, No. 1, pp. 520-522 (1 July 1991).

Tunneling stabilized magnetic force microscopy (TSMFM) is done with a scanning tunneling microscope (STM) having a flexible magnetic tip. TSMFM can be used to generate maps of magnetic records with submicrometer resolution. We find that Au-coated, Ni-film tips made from a free-standing 0.5-μm-thick Ni film can be used as a noninvasive probe for imaging magnetic bit patterns on the surfaces of a computer hard disk and floppy disks and computer tape. This variant of STM shows promise as a viable tool for diagnostic use in the magnetic recording industry.
[Contact: John Moreland, (303) 497-3641]

Rice, P., and Moreland, J., **Tunneling-Stabilized Magnetic Force Microscopy of Bit Tracks on a Hard Disk** [original title: Tunneling Stabilized Magnetic Force Microscopy], IEEE Transactions on Magnetics, Vol. 27, No. 3, pp. 3452-3454 (May 1991).

Tunneling stabilized magnetic force microscopy (TSMFM) is an elementary variation of scanning tunneling microscopy (STM). As in STM, a sharp conductive tip is scanned across a conductive sample with an electrical potential applied. As the tip is scanned, changes in tunneling current are plotted on a computer screen as a topographical image. The difference between STM and TSMFM is that the TSMFM tip is made from a flexible magnetic film which deflects in response to sample surface magnetic forces.

Pinning of the Abrikosov flux lattice in high-temperature superconductors determines the critical current. The application of TSMFM to image the Abrikosov flux lattice is presented. We present results of attempts to image sputter-deposited YBCO films above and below the critical temperature.
[Contact: Paul Rice, (303) 497-3541]

Superconductors

Released for Publication

Bray, S., and Ekin, J.W., **Critical-Current Degradation in Nb_3Sn Composite Wires Due to Locally Concentrated Transverse Stress**, to be published in the Proceedings of the International Cryogenic Materials Conference, Huntsville, Alabama, June 10-14, 1991.

The superconducting wires in an energized magnet coil are subjected to mechanical stresses caused by the Lorentz force. Previous measurements have shown that either axial tensile stress or transverse compressive stress, the two dominant stresses on the wire, can cause substantial degradation in the superconductor's critical current. The previous transverse stress measurements were made with uniformly applied stress; however, many superconductor applications employ cables where the strands experience stress concentrations at the points where they cross one another. For this study, a single stress concentration point was simulated by applying transverse stress to two Nb_3Sn wires, which were crossed over each other at an angle, while measuring the critical current of one of the wires at magnetic fields up to 9 T. A comparison between the cross-over-transverse-stress measurements and the uniform-transverse-stress measurements shows a critical-current degradation at equivalent loads that is significantly greater for the cross-over situation due to the reduced area. However, these preliminary data indicate that the concentration effect can be simply predicted because the degradation in critical current is comparable at equivalent stress.
[Contact: Steven Bray, (303) 497-5631]

Ekin, J.W., **Effect of Cable and Strand Twist Pitch Coincidence on the Critical Current of Flat, Coreless Superconductor Cables.**

We present data which indicate that a very simple technique of enhancing the critical current in flat, coreless superconductor cables is to match the cable twist pitch with the strand twist pitch. In this manner, the same group of filaments within each strand are degraded at each successive bend at the cable edges. This coincident-twist method minimizes current transfer among filaments, enhances the slope of the voltage-current characteristic, consistently improves

the critical current by about 10% in these tests, and is easy to apply.
[Contact: John W. Ekin, (303) 497-5448]

Ekin, J.W., Bray, S.L., Miller, T.A., Finnemore, D.K., and Tenbrink, J., **Uniaxial Strain Effect on the Transport Critical Current of Ag-Sheathed $Bi_2Sr_2Ca_1Cu_2O_{8+x}$ Superconductors.**

The first practical electromechanical properties of a high-T_c superconductor have been measured for Ag-sheathed $Bi_2Sr_2Ca_1Cu_2O_{8+x}$ superconductors at high magnetic fields up to 25 T. A melt-processed "powder in tube" $Bi_2Sr_2Ca_1Cu_2O_{8+x}$ conductor had an irreversible strain of 0.2% for the onset of permanent damage and a 50% critical-current-degradation strain of 0.36%. A discontinuous filament melt-processed Ag-sheathed $Bi_2Sr_2Ca_1Cu_2O_{8+x}$ superconductor was measured to have an irreversible strain of 0.6% and a 50% degradation strain of about 1%. These strain damage thresholds are about an order of magnitude higher than for high-T_c superconductors made by the bulk-sinter process and, for the first time, have reached the practical strain range for magnet design.
[Contact: John W. Ekin, (303) 497-5448]

Ishida, T., Goldfarb, R.B., Okayasu, S., and Kazumata, Y., **Static and Nonlinear Complex Susceptibility of $YBa_2Cu_3O_7$.**

We have investigated the harmonic susceptibility $\chi_n = \chi_n' - i\chi_n'$ (n = 1,2,3,...) of sintered $YBa_2Cu_3O_7$ in the field of $H_{dc} + H_{ac}\sin\omega t$. χ_1' and χ_1'' as functions of temperature depend on both H_{ac} and H_{dc}. Both even and odd χ_n's were detected for nonzero H_{dc}, but only odd harmonies were observed for zero H_{dc}. At constant temperature, χ_n is an even function of H_{dc} for n = odd, while χ_n is an odd function of H_{dc} for n = even. We compared experimental features with the prediction of the critical state model. For comparison, the static susceptibility χ_{dc} of $YBa_2Cu_3O_7$ was examined as a function of temperature. The $\chi_{dc}(T)$ curve for the zero-field-cooled sample has a two-step structure like χ_1'. However, $\chi_{dc}(T)$ for the sample cooled in small fields is unusual; a negative peak occurs near T_c, which can be explained by intragranular flux depinning upon warming.
[Contact: Ronald B. Goldfarb, (303) 497-3650]

Moreland, J., Dube, W.P., and Goodrich, L.F., **Dynamic Resistance of Superconducting $YBa_2Cu_3O_x$ Sintered Powder at 81 K: Liquid Versus Vapor Nitrogen Environment**, to be published in the Proceedings of the International Cryogenic Materials Conference, Huntsville, Alabama, June 10-14, 1991.

The dynamic resistance as a function of transport current in a superconducting $YBa_2Cu_3O_x$ sintered powder sample depends on its thermal surroundings. Plots of V versus I, measured with a nanovoltmeter, and dV/dI and d^2V/dI^2 versus I measured with a lock-in amplifier, are markedly different for the sample in nitrogen vapor compared to those measured in liquid nitrogen at 81 K. Assuming the usual power law dependence of $V = V_o[I/I_o]^n$, then $n = (I \times d^2V/dI^2)/dV/dI + 1$. Therefore, by measuring dV/dI and d^2V/dI^2 at a given current, the n factor can be determined for the V-I curve at that current. Plots of $(I \times d^2V/dI^2)/dV/dI$ as a function of I and dV/dI quantify the curvature of the V-I characteristics of the sample. At 81 K, we find that at the onset of detectable flux flow in the sample, the n factor determined from the dynamic derivatives of the V-I curve is 15 in the vapor versus 5 in the liquid. This phenomenon could be the basis for cryogenic flow meters, bolometers, level detectors, or other types of noninvasive, low-dissipation, thermal sensors.
[Contact: John Moreland, (303) 497-3641]

Moreland, J., Rice, P., Russek, S.E., Jeanneret, B., Roshko, A., Rudman, D.A., and Ono, R.H., **Scanning Tunneling Microscopy of the Surface Morphology of $YBa_2Cu_3O_x$ Thin-Films Between 300 K and 76 K.**

Scanning tunneling microscopy (STM) images of $YBa_2Cu_3O_x$ (YBCO) thin films show different growth habits depending on the deposition method and substrate material. In particular, we present images of YBCO films sputter deposited onto MgO and $SrTiO_3$ and laser ablated onto $LaAlO_3$. Both screw dislocation and ledge growth are observed. The STM morphology of YBCO films sputtered onto MgO substrates is investigated as a function of temperature. We find that at room temperature growth steps have an anomolously large apparent height which decreases with decreasing temperature, approaching the expected value for one unit cell of 1.2 nm at 76 K. Presumably, this phenomenon reflects changes in either the surface tunneling barrier or tunneling density of states upon cooling.
[Contact: John Moreland, (303) 497-3641]

Shi, D., Salem-Sugui, S., Jr., Wang, Z., Goodrich, L.F., Dou, S.X., Liu, H.K., Guo, Y.C., and Sorrell, C.C., **Critical Currents in Silver-Sheathed $(Bi,Pb)_2Sr_2Ca_2Cu_3O_{10-y}$ Superconducting Tapes.**

Nearly 95 vol% of the 110-K superconducting phase was formed by lead doping in a Bi-Sr-Ca-Cu-O system. The processed 110-K superconducting powders were used to produce long silver-sheathed tapes with a highly textured microstructure by rolling and prolonged sintering. The transport critical-current density was measured at 4.2 K to be 0.7×10^5 A/cm^2 at zero field and 1.6×10^4 A/cm^2 at 12 T for H parallel to the plane defined by the a and b axes. At 77 K, the critical-current density reached a value of $\sim 1 \times 10^4$ A/cm^2 at zero field for H parallel to the plane defined by the a and b axes and gradually decreased to 419 A/cm^2 at 1 T. Excellent grain alignment in the a-b plane led to a greatly improved critical-current density under a magnetic field. The relationship between the transport properties and the microstructure of the tapes is discussed.
[Contact: Loren F. Goodrich, (303) 497-3143]

Recently Published

Ekin, J.W., and Bray, S.L., **Effect of Transverse Stress on the Critical Current of Bronze-Process and Internal-Tin Nb_3Sn**, Journal of Applied Physics, Vol. 69, No. 8, pp. 4436-4438 (15 April 1991).

The effect of transverse stress on the measured critical current of two substantially different Nb_3Sn superconductors, a bronze-process conductor and an internal-tin conductor, has been measured. Photomicrographs of the two conductors reveal a basic difference in their microstructure. The bronze-process conductor exhibits columnar grains that are radially oriented within the Nb_3Sn filaments, while the grains of the internal-tin conductor are more equiaxed and randomly oriented. The radial orientation of the bronze-process grains defines an anisotropy between the axial and transverse directions that might account for the greater sensitivity of the critical current to transverse stress reported previously. The effect of transverse stress on the internal-tin conductor, however, is comparable to that of the bronze-process conductor. Thus, these data indicate that the transverse stress effect is not highly dependent on either grain morphology or fabrication process. From an engineering standpoint, the similarity of the transverse stress effect for these two types of Nb_3Sn superconductors represents an important simplification for setting first-order quantitative limits on the mechanical design of large superconducting magnets.
[Contact: John W. Ekin, (303) 497-5448]

Ekin, J.W., Salama, K., and Selvamanickam, V., **High-Transport Current Density Up to 30 T in Bulk $YBa_2Cu_3O_7$ and the Critical Angle Effect**, Applied Physics Letter, Vol. 59, No. 3, pp. 360-362 (15 July 1991).

Measurements of the dc transport critical current of oriented-grained $YBa_2Cu_3O_7$ have been made using high-quality Ag contacts and a high-current sample mount. The critical-current density J_c at 77 K for mutually perpendicular current and magnetic field B in the a,b plane is 8 kA/cm^2 at 8 T, decreasing gradually to 3.7 kA/cm^2 at 20 T, and remaining over 1 kA/cm^2 out to 30 T. High magnetic field measurements of J_c as a function of the angle θ of B with respect to the c axis are also reported. In contrast to earlier results at lower fields ($\leq$3 T), the measurements reported here in high fields reveal a J_c vs θ curve with a head-and-shoulders shape, consisting of a sharp peak ("head") $<5°$ wide for B parallel to the CuO_2 planes, and a wide (30° at 9 T, for example) shoulder region on either side of B$\perp$c axis, where the transport J_c remains high and constant. Beyond the shoulder region, however, the transport J_c decreases sharply, giving rise to the concept of a critical field angle for application design, defined by the minima in $d^2J_c/d\theta^2$ at the edge of the shoulders.
[Contact: John W. Ekin, (303) 497-5448]

Goodrich, L.F., **High-T_c Superconductor Voltage-Current Simulator and the Pulse Method of Measuring Critical Current**, Cryogenics, Vol. 31, pp. 720-727 (August 1991).

A passive voltage-current (V-I) simulator has been developed and tested using pulse-current and conventional direct-current methods. The simulator was designed to generate the extremely nonlinear V-I characteristic of a superconductor. It is intended to be used to test various components of the measurement system such as instrumentation, measurement method, and data analysis software to determine the transport critical current or critical current density of

a superconductor. Since this simulator does not emulate all of the subtle effects of a superconductor, it provides a necessary but not sufficient test of the measurement system. A comparison of preliminary results of the pulse-current and direct-current methods on the passive simulator is presented. Also, comparisons of methods using bulk and thin-film YBCO samples are given.
[Contact: Loren F. Goodrich, (303) 497-3143]

Moreland, J., Li, Y.K., Goodrich, L.F., Roshko, A., and Ono, R.H., **Novel Procedure for Mapping the J_c-H_{c2}-T_c Surface and Its Application to High Temperature Superconductors**, Science and Technology of Thin Film Superconductors 2, pp. 429-438 (Plenum Press, New York, 1990). [Proceedings of the Conference on Science and Technology of Thin Film Superconductors, Denver, Colorado, April 30-May 4, 1990).]

We have used an ac lock-in method for measuring the dynamic resistance versus current (dV/dI-I) curves to determine $J_c(T,H)$. The sample current consisted of a small constant oscillating current added to a variable dc current. The dc current was either slowly ramped for dV/dI-I measurements or controlled, keeping the dV/dI level constant while ramping temperature or field. In this way, it was possible to measure $J_c(T)$ at constant H. The temperature is controlled between 4 and 300 K using a bathysphere cryostat. The bathysphere cryostat was inserted into a high field magnet for measurements at fields up to 7 T. We have measured several high-temperature superconductors including YBCO thin films. In addition, we have measured the dV/dI-I curve of a simulator with a V-I curve having the form $V = 10\ \mu V \times (I/1.4\ A)^{13}$. Upon numerical integration, our data for the superconductors and the simulator are consistent with those obtained using a dc method using an analog nanovoltmeter to measure the V-I curves directly.
[Contact: John Moreland, (303) 497-3641]

Takagi, T., Chiang, Y.-M., and Roshko, A., **Origin of Grain Boundary Weak Links in $BaPb_{1-x}Bi_xO_3$ Superconductor** [original title: Origin of Grain Boundary Weak Links in $BaPb_{0.75}Bi_{0.25}O_3$ Superconductors], Journal of Applied Physics, Vol. 68, No. 11, pp. 5750-5758 (1 December 1990).

Although $BaPb_{0.75}Bi_{0.25}O_3$ (BPB) has a comparatively large superconducting coherence length of ~7 nm and no reported anisotropy in its superconducting parameters, polycrystalline BPB exhibits the same rapid decrease in transport critical-current density (J_{ct}) with low applied field (< ~5 Oe) that is characteristic of grain boundary weak-links in cuprate superconductors (e.g., $La_{2-x}Sr_xCuO_4$, $YBa_2Cu_3O_{7-x}$). We have studied the effects of processing thermal history on the formation and morphology of grain boundary phases, and on the chemistry of BPB boundaries with and without second phase, in order to understand the origin of these weak links. Scanning transmission electron microscopy and Auger electron spectroscopy results show the presence of a Pb-Bi-Ba-O phase that is wetting and liquid above ~570 °C, but which retracts to three-grain junctions upon slow cooling or annealing at lower temperatures. The composition of the grain boundaries as well as J_{ct} vs. temperature measurements suggest that the boundaries act as SIS tunnel junctions.
[Contact: Alexana Roshko, (303) 497-5420]

Other Electrical Systems Topics

Released for Publication

Thompson, C.A., and Fickett, F.R., **Electrical Resistivity of Copper Alloys Between 76 K and 300 K.**

The advent of high-temperature superconductivity and the recent interest in liquid-nitrogen-cooled magnets have increased interest in high-strength, high-conductivity materials in the temperature range 76 K to 300 K. We have measured the electrical resistivity of UNS C10100, C10200, C10700, C11000, C15715, and C17510 alloys at ten equally spaced temperatures over this range. Comparisons between alloys are made using measured resistivity and reported yield strengths. An apparatus which allows for accurate temperature control and simultaneous resistance measurement of eight samples is described.
[Contact: Curtis A. Thompson, (303) 497-5206]

Recently Published

Martzloff, F.D., and Perry, A.G., **Annotated Bibliography - Diagnostic Methods and Measurement Approaches to Detect Incipient Defects Due to Aging of Cables**, NIST 4485 (July 1991).

Open literature papers and some limited distribution

documents were reviewed in a search to identify promising approaches to the in-situ detection of incipient defects in nuclear power plant cables. The search was extended to the topics of detection of any defect, to radiation effects, and to basic considerations on partial discharges. This report presents a review of 150 papers that appeared significant from their title, but many of which were found not applicable upon close review. A compilation of 850 references cited in the reviewed papers is included in this paper.
[Contact: Francois D. Martzloff, (301) 975-2409]

ELECTROMAGNETIC INTERFERENCE

Conducted EMI

Released for Publication

Martzloff, F.D., **IEEE Guide on Surge Voltages Upgraded to Recommended Practice.**

After ten years of use as a guide, a revision has been completed and published as an IEEE Recommended Practice: Surge Voltages in Low-Voltage AC Power Circuits. This is an article to be published in a trade magazine circulated to writers, users, and enforcers of standards on electromagnetic compatibility, in order to give them a preview of the forthcoming IEEE document.
[Contact: Francois D. Martzloff, (301) 975-2409]

Recently Published

Martzloff, F.D., **Diverting Surges to Ground: Expectations Versus Reality**, Proceedings of the Open Forum on Surge Protection Application, Gaithersburg, Maryland, June 18-19, 1991, pp. 125-132 (1991).

A misconception is sometimes encountered that surges can be eliminated by sending them on a one-way trip to "ground" in a manner similar to leftovers that disappear in the kitchen sink disposal, never to be seen again. Unfortunately, electricity travels on closed loops, and no amount of "grounding" - be it dedicated, isolated, separated, or otherwise - can dispose of unwanted electrons. Sending them down the drain of a grounding conductor makes them reappear in a microsecond about 200 m away on some other conductor. The cycle for the waste through the environment takes longer, giving the illusion of disposal (at least as seen from the point of view of the kitchen sink - from the global point of view, one should take a different view, but that is another story). This paper presents a brief review of some of the fallacies, with illustrative measurement results, and proposes two approaches for remedy, rather than counterproductive grounding practices based on misconceptions.
[Contact: Francois D. Martzloff, (301) 975-2409]

Martzloff, F.D., **Testing Varistors Against the VDE 0160 Standard**, Proceedings of the Open Forum on Surge Protection Application, Gaithersburg, Maryland, June 18-19, 1991, pp. 81-88 (1991).

High-energy surge tests have been performed on metal-oxide varistors of a type in common use, according to a proposed IEC standard derived from German Standard VDE 0160. Depending on the position of the varistor within its tolerance band, failure or degradation can occur, validating the concern that this test requirement may be too severe for a universal application.
[Contact: Francois D. Martzloff, (301) 975-2409]

Radiated EMI

Released for Publication

Koepke, G.H., Driver, L.D., Cavcey, K.H., Masterson, K.D., Johnk, R., and Kanda, M., **A Standard Spherical Dipole Source**, to be published as NIST Technical Note 1351.

This report describes the development of a standard spherical dipole transmitter that operates from 10 to 1000 MHz. The report includes the complete electronic, mechanical, optical, and theoretical details that are necessary to construct this device and predict the electromagnetic fields which are radiated in simple environments.
[Contact: Galen H. Koepke, (303) 497-5766]

Recently Published

Crawford, M.L., and Ladbury, J.M., **Mode-Stirred Chamber for Measuring Shielding Effectiveness of Cables and Connectors: Assessing MIL-STD-1344A**

Method 3008, Connection Technology, pp. 45-51 (June 1989).

The mode-stirred method for measuring the shielding effectiveness (SE) of cables and connectors as specified in MIL-STD-1344A Method 3008 is examined. Problems encountered in applying the method are identified, and recommendations to improve the measurement results are provided. These include chamber design, type and placement of transmitting and reference receiving antenna, determination and correction for voltage standing-wave ratio of the reference antenna and equipment under test (EUT), and the measurement approach to use at specified test frequencies. Design and measurement setups for a small mode-stirred chamber suitable for performing SE measurements in the frequency range 1 to 18 GHz with dynamic ranges up to 130 dB are given along with SE measurement results of some sample EUTs.
[Contact: Myron L. Crawford, (303) 497-5497]

Hill, D.A., **Diffraction by a Half-Plane in a Lossy Medium**, Journal of Applied Physics, Vol. 69, No. 12, pp. 8405-8407 (15 June 1991).

The classical problem of plane-wave diffraction by half plane is extended to allow for loss in the surrounding medium. The loss causes the arguments of the integral functions to become complex. Numerical results show that the relative importance of the edge-diffracted field decreases as the loss is increased. This effect is important in interpreting the effects of off-path scatterers in remote sensing of lossy media. The results for both electric and magnetic polarizations are in qualitative agreement with previous results based on the Kirchhoff approximation.
[Contact: David A. Hill, (303) 497-3472]

Randa, J., Kanda, M., and Orr, R.D., **Resistively-Tapered-Dipole Electric-Field Probes up to 40 GHz**, Proceedings of the IEEE 1991 International Symposium on Electromagnetic Compatibility, Cherry Hill, New Jersey, August 12-16, 1991, pp. 265-266 (1991).

We have developed an electric-field probe for use as a transfer standard at frequencies up to 40 GHz. The lower frequency cutoff is below 1 MHz. The design is based on the resistively-tapered-dipole (RTD) probes developed for frequencies up to 18 GHz. Those probes used 8-mm tapered dipoles. In this work, we have used 6-, 4- and 2-mm dipoles to extend the frequency range. Because the new probes are isotropic, have relatively flat frequency response, and have a response which drops off outside their operating frequency range, they could also be used as hazard meters.
[Contact: James P. Randa, (303) 497-3150]

Randa, J.P., Kanda, M., and Orr, R.D., **Thermo-Optic Designs for Electromagnetic-Field Probes for Microwaves and Millimeter Waves**, IEEE Transactions on Electromagnetic Compatibility, Vol. 33, No. 3, pp. 205-214 (August 1991).

We report the development of an electromagnetic-field probe for microwave and millimeter-wave frequencies. The probe uses an optically sensed thermometer to measure the heating of a resistive element in an electromagnetic field. The response is calculated for several different configurations of the resistive element, and two optimal designs are chosen. Measurements on experimental probes of these designs are presented. One of the designs displays a flat frequency response above 30 GHz and a sensitivity of 38 V/m. We identify improvements in the design which should significantly increase the sensitivity and improve the low-frequency response.
[Contact: James P. Randa, (303) 497-3150]

ADDITIONAL INFORMATION

Lists of Publications

DeWeese, M.E., **Metrology for Electromagnetic Technology: A Bibliography of NIST Publications**, NISTIR 3972 (August 1991).

This bibliography lists the publications of the personnel of the Electromagnetic Technology Division of NIST in the period from January 1970 through publication of this report. A few earlier references that are directly related to the present work of the Division are included.
[Contact: Sarabeth Moynihan, (303) 497-3678]

Lyons, R.M., and Gibson, K.A., **A Bibliography of the NIST Electromagnetic Fields Division Publications**, NISTIR 3973 (August 1991).

This bibliography lists publications by the staff of the

National Institute of Standards and Technology's Electromagnetic Fields Division for the period from January 1970 through August 1991. Selected earlier publications from the Division's predecessor organizations are included.
[Contact: Kathryn A. Gibson, (303) 497-3132]

Palla, J.C., and Meiselman, B., **Electrical and Electronic Metrology: A Bibliography of NIST Electricity Division's Publications, NIST List of Publications 94** (January 1992).

This bibliography covers publications of the Electricity Division, Electronics and Electrical Engineering Laboratory, NIST, and of its predecessor sections for the period January 1968 to December 1991. A brief description of the Division's technical program is given in the introduction.
[Contact: Jenny C. Palla, (301) 975-2220]

Walters, E.J., **Semiconductor Measurement Technology, NIST List of Publications 72** [a bibliography of NIST publications concerning semiconductor measurement technology for the years 1962-1989] (March 1990), and **LP72 Supplement, Publications for the Year 1990** (April 1991).

The bibliography contains reports of work performed at the National Institute of Standards and Technology in the field of Semiconductor Measurement Technology in the period from 1962 through December 1990. An index by topic area and a list of authors are provided. The supplement provides information on technology transfer at NIST for calendar year 1990, not only from those groups specializing in semiconductor electronics, but also including NIST-wide research now coordinated by the NIST Office of Microelectronics Programs.
[Contact: E. Jane Walters, (301) 975-2050]

New NIST Research Material

NIST has announced the availability of **Research Material 8458**, a well-characterized artificial flaw used as an **artifact standard in eddy current nondestructive evaluation (NDE)**. The new Research Material (RM) is the outcome of work carried out by the Electromagnetic Technology Division to address the need for calibration standards for eddy-current NDE, for example, as used to detect fatigue cracks in aircraft structures. The RM flaw is produced in an annealed aluminum alloy block by first indenting the block and then compressively deforming the resulting notch until it is tightly closed. The next operation is to restore a flat finish to the block face, after which the block is heat treated to the original temper. The controlled flaw has been named the "CDF notch," after its inventors (listed on patent application) Thomas E. Capobianco (Electromagnetic Technology Division), William P. Dube (Division 832), and Ken Fizer (Naval Aviation Depot, NAS Norfolk, Virginia).

In the past, the challenge has been to manufacture artificial flaws that closely simulate the mechanical properties of fatigue cracks. Currently used artifacts include electrical-discharge-machined and saw-cut notches, both of which are relatively poor representations of fatigue cracks as their widths are too great. The Division-developed method provides notches that can be made controllably in a variety of geometries, have known dimensions, with widths that are narrow enough to provide an acceptable representation of fatigue cracks.

An NIST Research Material is not certified by NIST, but meets the International Standards Organization definition of "a material or substance one or more properties of which are sufficiently well established to be used in the calibration of an apparatus, the assessment of a measurement method, or for assigning values to materials." The documentation issued with RM 8458 is a "Report of Investigation." Contact: technical information — Fred Fickett, (303) 497-3785; order information — Standard Reference Materials Program, (301) 975-6776.

Continuing Production-Expanded-Capability Standard Reference Materials

The Semiconductor Electronics Division announces the continuing production of three thicknesses and the addition of two new thicknesses for the Standard Reference Material (SRM) for **ellipsometrically derived thickness and refractive index of a silicon dioxide film on silicon.** For sale to the public through the NIST Standard Reference Material Program Office [(301) 975-6776], the following three individual oxide thicknesses continue to be available: 50 nm

(SRM 2531), 100 nm (SRM 2532), and 200 nm (SRM 2533). Recently, two new thicknesses, 25 nm (SRM 2534) and a limited number of 14-nm prototypes (SRM 2535), were added to the availability list.

SRMs 2531, 2532, and 2533, originally released as SRM 2530-1, 2530-2, and 2530-3, were developed in response to the industry's need to evaluate the accuracy of ellipsometers and other thin-film thickness-monitoring instruments. The scope of these SRMs has now expanded with the recent issuance of the 25-nm and 14-nm oxide thicknesses so they have application as thickness standards for use in research as well as in semiconductor fabrication production lines.

Each SRM unit, consisting of a 76-mm (3-in) diameter silicon wafer on which a uniform silicon dioxide layer has been grown, is individually measured and certified over a 5-mm diameter area in the center of the wafer for the ellipsometric parameters delta, Δ, and psi, ψ, at the vacuum wavelength λ = 633.0 nm using the High-Accuracy Ellipsometer built at NIST. Each SRM is also certified for the derived values for the thicknesses and indices of refraction of both layers of a two-layer optical model of an oxide film on a single-crystal silicon substrate.
[Contact: Barbara J. Belzer, (301) 975-2248]

Recently Issued Standard Reference Materials

The Microelectronics Dimensional Metrology Group of the Precision Engineering Division announces the release of two Standard Reference Materials (SRMs) for calibrating optical microscopes used to measure linewidths on photomasks. Each SRM consists of a 63.5 × 63.5 × 1.5 mm (2.5 × 2.5 × 0.060 in) photomask patterned with chromium lines of widths in the range of 0.9 to 10.8 µm. SRM 475, patterned with antireflecting chromium on a quartz substrate, is being reissued after being out of production for almost four years. SRM 476, a new SRM, is patterned with bright chromium on a borosilicate substrate.

In addition to isolated opaque lines on a clear background and isolated clear lines on an opaque background, these SRMs contain opaque line pairs for calibrating the length scale of optical microscopes, adjacent clear and opaque lines of approximately equal widths for setting the line-to-space ratio (contrast) on video image-scanning instruments, and features with 10 approximately equally spaced opaque lines for checking the linearity of measurement systems (e.g., the magnification as a function of position over the field of view).

The certified linewidth and spacing values were determined from measurements made with the NIST automated linewidth measurement system. The uncertainty of the linewidth measurements is 0.081 µm or less for SRM 475 and 0.064 µm or less for SRM 476. The dominant contribution to this uncertainty is the nonvertical geometry of the line edges, and finding a source of photomasks with better edge geometry would lead to considerable improvement in the calibration uncertainty.
[Contact: James E. Potzick, (301) 975-3481 or Robert D. Larrabee, (301) 975-2298]

Emerging Technologies in Electronics ... and Their Measurement Needs, Second Edition

This report assesses the principal measurement needs that must be met to improve U.S. competitiveness in emerging technologies within several fields of electronics: semiconductors, superconductors, magnetics, optical fiber communications, optical fiber sensors, lasers, microwaves, video, and electromagnetic compatibility. The report seeks feedback from industry and Government agencies on the assessment. The feedback will guide the development of NIST programs that provide U.S. industry with new documented measurement methods, new national reference standards to assure the accuracy of those measurement methods, and new reference data for electronic materials. Copies may be obtained by ordering Report No. PB90-188087/AS ($23.00 hard copy, $11.00 microfiche) from the National Technical Information Service, 5285 Port Royal Road, Springfield, VA 22161, (703) 487-4650.

Transfer of Pulse Waveform Measurements Services to NIST, Gaithersburg, MD

The responsibility for the Special Test services provided by NIST for pulse waveform measurements has now been officially transferred to the Electricity Division, Electronic Instrumentation and Metrology Group (811.02) in Gaithersburg, MD. These services include:

Test Number	Description of Services
65100S	Impulse Generator Spectrum Amplitude (50 Ohm)
65200S	Fast Repetitive Broadband Pulse Parameters (50 Ohm)
65300S	Network Impulse Response (S_{21}) of Coaxial Networks
65400S	Pulse Time Delay through Coaxial Transmission Lines

Service for test number 65400S is already available; it is anticipated that the equipment and software necessary for bringing the other waveform measurement services on line will also become available by June 30, 1992. Please direct specific technical questions concerning these services to Mr. William L. Gans, (301) 975-2502.

1992 EEEL CALENDAR

April 23-24, 1992 (Boston, Massachusetts)

Ion Implant Users Group Meeting. Sponsored by NIST, the next regular meeting will be expanded to two days. Topics to be discussed on the first day are: parallelism and high angle implant; artificial intelligence and implantation; and discussion of uptime calculation. Visits to Eaton, Varian, and Genus facilities are scheduled for the second day of the meeting. Preregistration is required.
[Contact: John Albers, (301) 975-2075]

June 24-26, 1992 (Stockholm, Sweden)

11th Workshop on VLSI Packaging Techniques and Manufacturing Technologies. The IEEE CHMT Society and NIST are co-sponsoring this 11th Workshop. Featured will be the design and implementation of electronic packaging and the technologies and equipment for high-frequency and high-density applications using single-chip packages and multichip modules.
[Contact George G. Harman, (301) 975-2097]

November 9-10, 1992 (Austin, Texas)

Workshop on Process Control Measurements for Advanced IC Manufacturing. In conjunction with SEMICON Southwest, the workshop, cosponsored by ASTM, JEIDA, JESSI, NIST, SEMATECH, SEMI, and SRC, will begin with overviews of the status of process control measurements in silicon device fabrication. Working sessions will consider the critical process control measurement issues in the following areas: film deposition, contamination, implant, etching, oxidation/diffusion, lithography, and materials. Standards development meetings will be held concurrently by ASTM Committee F-1 on Electronics and a selected number of SEMI Standards committees.
[Contact Robert I. Scace, (301) 975-4400]

EEEL SPONSORS

National Institute of Standards and Technology
U.S. Air Force
Hanscom Field; McClelland Air Force Base; Newark Air Force Station; Rome Air Development Center; Space & Missile Organization; Wright-Patterson Air Force Base; Secretary of the Air Force, Office of Research; SAF/FMBMB, Pentagon
U.S. Army
Army Aviation Systems Command; Dugway Proving Ground; Fort Belvoir; Fort Huachuca; Harry Diamond Laboratory; Materials & Mechanics Research Center; Redstone Arsenal; Strategic Defense Command; The Pentagon
Department of Commerce
NOAA; Census
Department of Defense
Advanced Research Projects Agency; Defense Nuclear Agency; Combined Army/Navy/Air Force (CCG); National Security Agency
Department of Energy
Energy Systems Research; Fusion Energy; Basic Energy Sciences; High Energy & Nuclear Physics
Department of Justice
Law Enforcement Assistance Administration; FBI
U.S. Navy
David Taylor Research Center; Naval Sea Systems Command; Weapons Support Center/Crane; Office of Naval Research; Naval Ship Research Development Center; Naval Air Systems Command; Naval Air Engineering Center; Aviation Logistics Center/Patuxent; Naval Explosive Ordnance Disposal Tech. Center; Naval Research Laboratory, Naval Aviation Depot, Naval Ocean Systems

Center; Naval Air Test Center; Indian Head
National Science Foundation
National Aeronautics and Space Administration
NASA Headquarters; Goddard Space Flight Center; Lewis Research Center
Nuclear Regulatory Commission
Department of Transportation
National Highway Traffic Safety Administration
MIMIC Consortium
Various Federal Government Agencies

NIST-114A
(REV. 3-90)

U.S. DEPARTMENT OF COMMERCE
NATIONAL INSTITUTE OF STANDARDS AND TECHNOLOGY

BIBLIOGRAPHIC DATA SHEET

1. PUBLICATION OR REPORT NUMBER
NISTIR 4726

2. PERFORMING ORGANIZATION REPORT NUMBER

3. PUBLICATION DATE
February 1992

4. TITLE AND SUBTITLE

Electronics and Electrical Engineering Laboratory Technical Progress Bulletin Covering Laboratory Programs, July to September 1991, with 1992 EEEL Events Calendar

5. AUTHOR(S)

J. A. Gonzalez, compiler

6. PERFORMING ORGANIZATION (IF JOINT OR OTHER THAN NIST, SEE INSTRUCTIONS)

U.S. DEPARTMENT OF COMMERCE
NATIONAL INSTITUTE OF STANDARDS AND TECHNOLOGY
GAITHERSBURG, MD 20899

7. CONTRACT/GRANT NUMBER

8. TYPE OF REPORT AND PERIOD COVERED
July-September 1991

9. SPONSORING ORGANIZATION NAME AND COMPLETE ADDRESS (STREET, CITY, STATE, ZIP)

10. SUPPLEMENTARY NOTES

All technical information included in this document has been approved for publication previously.

11. ABSTRACT (A 200-WORD OR LESS FACTUAL SUMMARY OF MOST SIGNIFICANT INFORMATION. IF DOCUMENT INCLUDES A SIGNIFICANT BIBLIOGRAPHY OR LITERATURE SURVEY, MENTION IT HERE.)

This is the thirty-sixth issue of a quarterly publication providing information on the technical work of the National Institute of Standards and Technology, Electronics and Electrical Engineering Laboratory. This issue of the EEEL Technical Progress Bulletin covers the third quarter of calendar year 1991. Abstracts are provided by technical area for both published papers and papers approved by NIST for publication.

12. KEY WORDS (6 TO 12 ENTRIES; ALPHABETICAL ORDER; CAPITALIZE ONLY PROPER NAMES; AND SEPARATE KEY WORDS BY SEMICOLONS)

antennas; electrical engineering; electrical power; electromagnetic interference; electronics; instrumentation; laser; magnetics; microwave; optical fibers; semiconductors; superconductors

13. AVAILABILITY

X	UNLIMITED
	FOR OFFICIAL DISTRIBUTION. DO NOT RELEASE TO NATIONAL TECHNICAL INFORMATION SERVICE (NTIS).
	ORDER FROM SUPERINTENDENT OF DOCUMENTS, U.S. GOVERNMENT PRINTING OFFICE, WASHINGTON, DC 20402.
X	ORDER FROM NATIONAL TECHNICAL INFORMATION SERVICE (NTIS), SPRINGFIELD, VA 22161.

14. NUMBER OF PRINTED PAGES
39

15. PRICE
A03

ELECTRONIC FORM

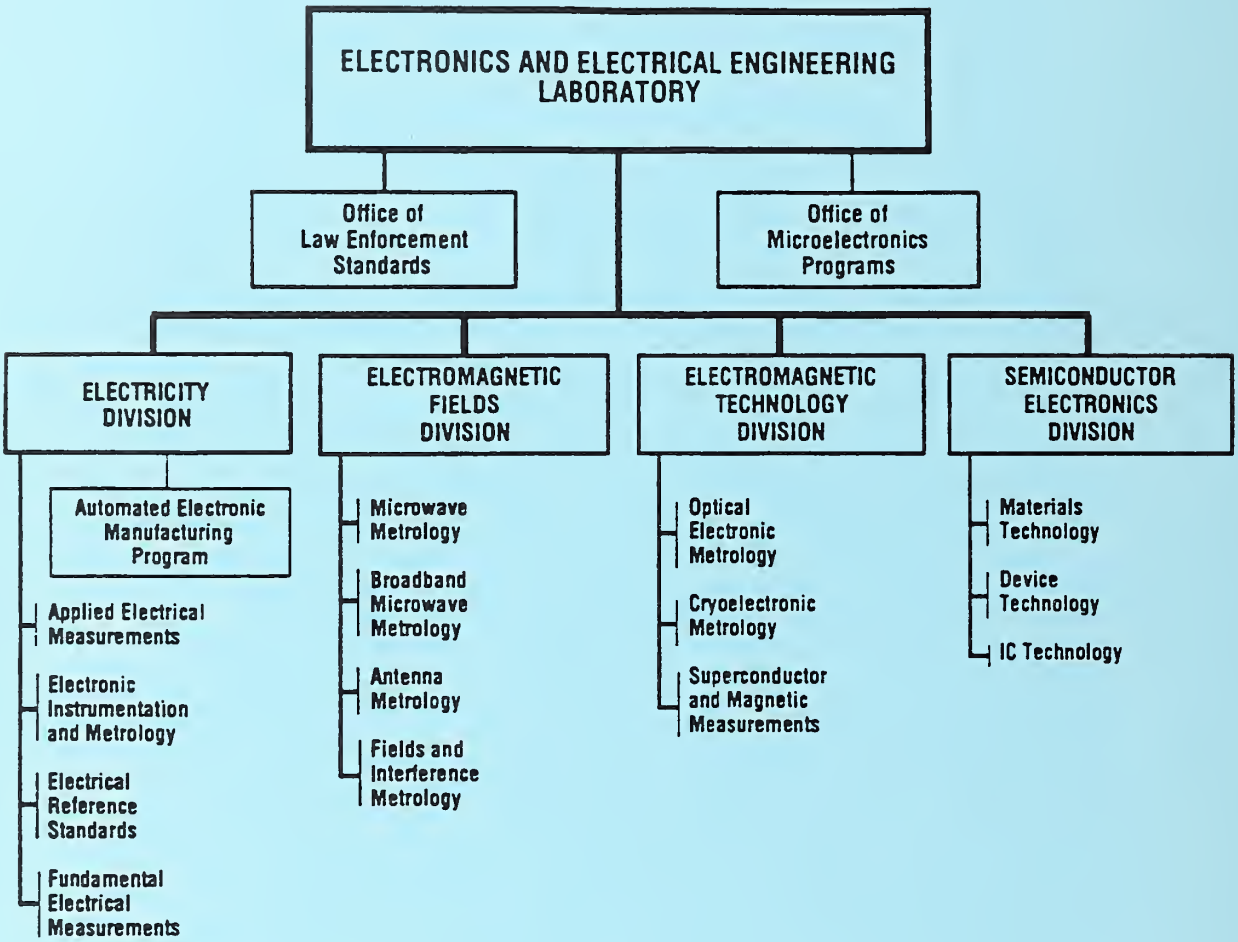

KEY CONTACTS

Laboratory Headquarters (810)	Director, Mr. Judson C. French (301) 975-2220
	Deputy Director, Dr. Robert E. Hebner (301) 975-2220
Office of Microelectronics Programs	Director, Mr. Robert I. Scace (301) 975-4400
Office of Law Enforcement Standards	Director, Mr. Lawrence K. Eliason (301) 975-2757
Electricity Division (811)	Chief, Dr. Oskars Petersons (301) 975-2400
Semiconductor Electronics Division (812)	Chief, Mr. Frank F. Oettinger (301) 975-2054
Electromagnetic Fields Division (813)	Chief, Dr. Ramon C. Baird (303) 497-3131
Electromagnetic Technology Division (814)	Chief, Dr. Robert A. Kamper (303) 497-3535

INFORMATION:

For additional information on the Electronics and Electrical Engineering Laboratory, write or call:

Electronics and Electrical Engineering Laboratory
National Institute of Standards and Technology
Metrology Building, Room B-358
Gaithersburg, MD 20899
Telephone: (301) 975-2220